U.S. Department of Transportation

Federal Railroad Administration

Full-Scale Rollover Test and Corresponding Analytical Modeling – Survivability of Top Fittings for a CPC-1232 Tank Car

Office of Research,
Development
and Technology
Washington, DC 20590

DOT/FRA/ORD-20/22

Final Report
May 2020

REPORT DOCUMENTATION PAGE

Form Approved
OMB No. 0704-0188

1. AGENCY USE ONLY (Leave blank)	2. REPORT DATE	3. REPORT TYPE AND DATES COVERED
	May 2020	Technical Report, 2015-2018

4. TITLE AND SUBTITLE
Full-Scale Rollover Test and Corresponding Analytical Modeling – Survivability of Top Fittings for CPC-1232 Tank Car

5. FUNDING NUMBERS

6. AUTHOR(S)
Robert Trent, Anand Prabhakaran, Florentina Gantoi, Vinaya Sharma

7. PERFORMING ORGANIZATION NAME(S) AND ADDRESS(ES)
Sharma & Associates, Inc.
5810 S Grant Street
Hinsdale, IL 60521

8. PERFORMING ORGANIZATION REPORT NUMBER

9. SPONSORING/MONITORING AGENCY NAME(S) AND ADDRESS(ES)
U.S. Department of Transportation
Federal Railroad Administration
Office of Railroad Policy and Development
Office of Research, Development and Technology
Washington, DC 20590

10. SPONSORING/MONITORING AGENCY REPORT NUMBER
DOT/FRA/ORD-20/22

11. SUPPLEMENTARY NOTES
COR: Francisco González, III

12a. DISTRIBUTION/AVAILABILITY STATEMENT
This document is available to the public through the FRA eLibrary.

12b. DISTRIBUTION CODE

13. ABSTRACT (Maximum 200 words)

A full-scale rollover test was performed on a CPC-1232 tank car body to determine the survivability of the top fittings and provide a comparison to past tank car-type rollover tests. Dynamic simulations were performed prior to the test to determine appropriate test conditions and parameters. Pivoting the carbody in a fixture about a fixed axis controlled the test conditions. The test was designed so that the manway bonnet, the highest profile top fitting, impacted a concrete target pad at 7.8 mph. As a result of the impact, the manway bonnet sheared off at its fasteners, several fasteners securing the pressure plate cover failed, and the unloading/loading valves sheared off. This resulted in a lading release. Post-test, the analytical simulation was correlated against the test results. Researchers recommend that methods to avoid the "unzipping" failures of bolted connections be considered for future designs. Alternatively, the observed failure mechanism may be incorporated into the design/specification process.

14. SUBJECT TERMS
Full-scale testing, fittings, protection, rollover, tank car, tank car safety, CPC-1232 car

15. NUMBER OF PAGES
44

16. PRICE CODE

17. SECURITY CLASSIFICATION OF REPORT	18. SECURITY CLASSIFICATION OF THIS PAGE	19. SECURITY CLASSIFICATION OF ABSTRACT	20. LIMITATION OF ABSTRACT
Unclassified	Unclassified	Unclassified	

NSN 7540-01-280-5500
Standard Form 298 (Rev. 2-89)
Prescribed by ANSI Std. 239-18
298-102

METRIC/ENGLISH CONVERSION FACTORS

ENGLISH TO METRIC

LENGTH (APPROXIMATE)

1 inch (in)	=	2.5 centimeters (cm)
1 foot (ft)	=	30 centimeters (cm)
1 yard (yd)	=	0.9 meter (m)
1 mile (mi)	=	1.6 kilometers (km)

AREA (APPROXIMATE)

1 square inch (sq in, in^2)	=	6.5 square centimeters (cm^2)
1 square foot (sq ft, ft^2)	=	0.09 square meter (m^2)
1 square yard (sq yd, yd^2)	=	0.8 square meter (m^2)
1 square mile (sq mi, mi^2)	=	2.6 square kilometers (km^2)
1 acre = 0.4 hectare (he)	=	4,000 square meters (m^2)

MASS - WEIGHT (APPROXIMATE)

1 ounce (oz)	=	28 grams (gm)
1 pound (lb)	=	0.45 kilogram (kg)
1 short ton = 2,000 pounds (lb)	=	0.9 tonne (t)

VOLUME (APPROXIMATE)

1 teaspoon (tsp)	=	5 milliliters (ml)
1 tablespoon (tbsp)	=	15 milliliters (ml)
1 fluid ounce (fl oz)	=	30 milliliters (ml)
1 cup (c)	=	0.24 liter (l)
1 pint (pt)	=	0.47 liter (l)
1 quart (qt)	=	0.96 liter (l)
1 gallon (gal)	=	3.8 liters (l)
1 cubic foot (cu ft, ft^3)	=	0.03 cubic meter (m^3)
1 cubic yard (cu yd, yd^3)	=	0.76 cubic meter (m^3)

TEMPERATURE (EXACT)

[(x-32)(5/9)] °F = y °C

METRIC TO ENGLISH

LENGTH (APPROXIMATE)

1 millimeter (mm)	=	0.04 inch (in)
1 centimeter (cm)	=	0.4 inch (in)
1 meter (m)	=	3.3 feet (ft)
1 meter (m)	=	1.1 yards (yd)
1 kilometer (km)	=	0.6 mile (mi)

AREA (APPROXIMATE)

1 square centimeter (cm^2)	=	0.16 square inch (sq in, in^2)
1 square meter (m^2)	=	1.2 square yards (sq yd, yd^2)
1 square kilometer (km^2)	=	0.4 square mile (sq mi, mi^2)
10,000 square meters (m^2)	=	1 hectare (ha) = 2.5 acres

MASS - WEIGHT (APPROXIMATE)

1 gram (gm)	=	0.036 ounce (oz)
1 kilogram (kg)	=	2.2 pounds (lb)
1 tonne (t)	=	1,000 kilograms (kg)
	=	1.1 short tons

VOLUME (APPROXIMATE)

1 milliliter (ml)	=	0.03 fluid ounce (fl oz)
1 liter (l)	=	2.1 pints (pt)
1 liter (l)	=	1.06 quarts (qt)
1 liter (l)	=	0.26 gallon (gal)
1 cubic meter (m^3)	=	36 cubic feet (cu ft, ft^3)
1 cubic meter (m^3)	=	1.3 cubic yards (cu yd, yd^3)

TEMPERATURE (EXACT)

[(9/5) y + 32] °C = x °F

QUICK INCH - CENTIMETER LENGTH CONVERSION

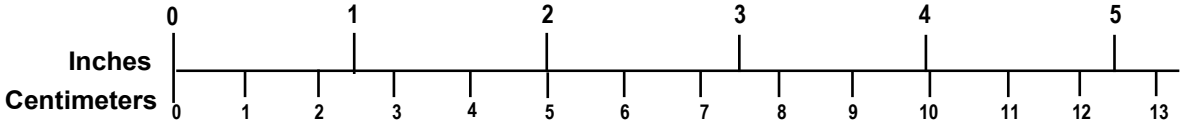

QUICK FAHRENHEIT - CELSIUS TEMPERATURE CONVERSION

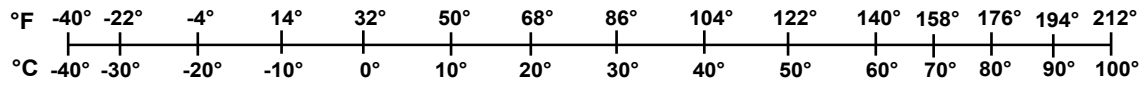

For more exact and or other conversion factors, see NIST Miscellaneous Publication 286, Units of Weights and Measures. Price $2.50 SD Catalog No. C13 10286

Updated 6/17/98

Contents

Table of Figures

Executive Summary

Railroad tank cars are normally outfitted with appurtenances located on top of the car that are used for loading/unloading and other functions. These fittings, which normally protrude outside the tank envelope, are apt to impact the ground or other objects during a rollover derailment. The survivability of these fittings in an unprotected state is questionable. Damage to the fittings will likely result in a release of lading and possibly a public hazard. The Federal Railroad Administration (FRA) has studied these risks and risk mitigation opportunities through analytical work and full-scale testing of non-pressure tank cars in the past. This report presents FRA-sponsored research conducted by Sharma & Associates, Inc., from 2015 to 2018, which evaluated the susceptibility of newer-specification top fittings protective structures on CPC-1232 cars through simulations and full-scale rollover testing.

Prior to testing, the Sharma research team performed FEA analysis using LS-DYNA, simulating the full-scale rollover test of the selected CPC-1232 car. This determined the correct concrete target location and orientation to obtain the agreed impact speed of 8.5 mph at the top fittings.

The team performed the test by placing the test article tank car body in the engineered rollover fixture with the carbody pinned at the bolsters of one side of the car. The carbody was free to rotate about this constraint. The apparatus was designed to push the carbody using hydraulic jacks to the point where it rolled off by gravity. The carbody was filled with water to simulate lading. Researchers designed the test setup so that the fittings impacted a concrete target pad at a desired impact speed. A high-speed video camera, strain gauges, and accelerometers were used to collect data. The test and approach followed a methodology developed earlier. This time the test was focused on cars that had been built to an upgraded standard.

A crude oil CPC-1232 car with the typical single manway loading/un-loading nozzle was used in the test. Researchers designed the test so that the protective bonnet of the fittings first impacted the concrete target block.

As a result of the impact, the manway bonnet sheared off at its fasteners, several fasteners securing the pressure plate cover failed, and the unloading/loading valves sheared off. This resulted in a lading release.

The team fine-tuned the FEA simulations after the test to improve correlation between the FEA simulation work and the full-scale test results. The post-test simulation agreed well with the actual test, showing similar results.

A key reason behind the failure seen during the test was the sequential failure of bolts at the pressure plate and bonnet. The bolted connection between the bonnet and the flange is designed so the bolts are loaded uniformly; however, under actual impact conditions the load distribution is not uniform, leading to an “unzipping” effect and separation of the bonnet from the flange.

The research team recommends that the potential for such sequential bolt failure, and mechanisms to improve the bolted connection be considered in the design of fittings protection. Alternately, one may consider incorporating that failure mechanism into the design and specification process. Additionally, the use of energy absorbing elements in the load path might better distribute the bolt loads resulting in an increased likelihood of survival.

1. Introduction

1.1 Background

Railroad tank cars use multiple valves, fittings, and other devices to allow efficient loading and unloading operations and to provide for the safe handling and transportation of lading. These include manways, liquid/vapor valves, pressure relief devices, vacuum relief devices, unloading valves, sample lines, gauging devices, and bottom outlets, that are generally installed on either the top or bottom of the car, based on the intended function of the device. The fittings generally project out of the envelope of the tank for easy access and are designed to provide safe operation under normal operating conditions.

Under serious derailment conditions, it is possible for one of these devices to impact the ground or another object resulting in structural failure of the device or the connection between the device and the tank, resulting in a leak or loss of lading of a hazardous material. The safety and environmental implications of such an event are tremendous.

Previous work in this area has focused on DOT 111 class non-pressure cars of pre-CPC-1232 specification vintage with both analytical simulation and full-scale testing. Tank cars built under the CPC-1232 and later specifications attempt to protect susceptible fittings within protective bonnets or other structures to reduce their susceptibility to rollover derailment caused failures. This study evaluates the improved levels of fittings protection on CPC-1232 tank cars through detailed FEA simulations and full-scale testing.

There are several structural differences relevant to this study between general service tank cars of the pre-CPC 1232 specification (previously tested DOT111s), the CPC-1232 specification, and the new current DOT 117 specification (yet to be tested), as provided in the available AAR MSRP C-III standards, circular letters, and DOT rule RIN 2137-AE91. Table 1-1 shows a summary of these relevant differences.

Table 1-1. Comparison of Relevant Tank Car Requirements

CAR TYPE	SPECIFICATION	TOP FITTINGS PROTETION	SHELL THICKNESS	TANK MATERIAL
PRE-CPC-1232 DOT 111	AAR M-1002 2007 release	Not required. When equipped per AAR specifications for Tank Cars app. E para. 10.2.1 (Pre-2007 release) Load: 2W Vertical 1W Horizontal	7/16”	TC-128 Grade B normalized

CAR TYPE	SPECIFICATION	TOP FITTINGS PROTETION	SHELL THICKNESS	TANK MATERIAL
CPC-1232 DOT 111	AAR M-1002 2007 or 2014 release depending on built date	Must be equipped per AAR Spec for Tank Cars App E. para 10.2.1 Load: 2W Vertical 1W Horizontal Or 1/2 W Vertical 1W Horizontal 1/2W Lateral (depending on built date)	1/2”	TC-128 Grade B normalized
DOT 117	DOT RIN 2137-AE91	Must be equipped per AAR Spec for Tank Cars App E. para 10.2.1 (2014 release) Load: 1/2 W Vertical 1W Horizontal 1/2W Lateral	9/16”	TC-128 Grade B normalized

2.5.2.3 Class DOT/TC-111 cars with carbon steel tanks must meet one of the following minimum criteria:

- Tanks are constructed of normalized TC128 steel at least 7/16 in. thick and equipped with steel jackets and 1/2 in. thick steel jacket heads.
- Tanks are constructed of normalized TC128 steel at least 1/2 in. thick and equipped with 1/2 in. thick steel half-head shields.
- Tanks are constructed of normalized ASTM A516 steel at least 1/2 in. thick and equipped with steel jackets and 1/2 in. thick steel jacket heads.
- Tanks are constructed of normalized ASTM A516 steel at least 5/8 in. thick and equipped with 1/2 in. thick steel half-head shields.

Figure 1-1. Section 2.5.2.3 from AAR MSRP C-III [M-1002]

1.2 Objectives

The key objectives of this effort were as follows:

1. Evaluate the performance of CPC-1232 car top fittings protection in a rollover scenario through analytical simulations and the test methodology adopted in prior FRA tests.
2. Determine strains, forces, and deflections seen by the fittings, local tank shell, and protective structure during the rollover.
3. Correlate test results with the analytical simulations, and identify opportunities for improvement.

1.3 Overall Approach

Prior work on analysis, simulations, and testing focused on non-pressure tank cars of pre-CPC-1232 standards (DOT111s). This study focused on the top fittings protection performance of CPC-1232 standard cars and used a CPC-1232 specification car used in crude oil service as the test car.

The technical approach was to:

- Model and simulate the expected performance of the fittings protective structure on the specimen CPC-1232 car under the FRA test conditions.
- Identify the expected impact speed at which fittings protection may be compromised; this becomes the target impact speed for the test effort.
- Instrument the specimen car and set up the test for the target impact speed.
- Conduct the test, observe the results, and gather relevant data for the model correlation effort.
- Fine-tune model performance to match the observed test performance.
- Recommend opportunities for improvement.

1.4 Organization of the Report

The report is organized as follows:

- Section 2 describes the test article.
- Section 3 provides an overview of the test setup.
- Section 4 describes the details of the test setup.
- Section 5 describes the test results.
- Section 6 describes the FEA modeling.

2. Test Article

The tank car available for this test was the Trinity built BRGX 0942 (Figure 2-1). These cars are 31,808-gallon crude oil service cars of AAR class DOT111A100W1. They have a lightweight of 74,800 lbs, a load limit of about 211,200 lbs, and a truck center spacing of 45'-10¼". The car is equipped with a common crude oil car fittings arrangement. This includes a vacuum release valve, a loading valve, a vent valve, and a safety valve. These valves are shown in Figure 2-2. For this test, the total test article weight (carbody minus trucks filled to a 20 percent outage with water) was 266,000 lbs. Since water has a higher specific weight than crude oil (8.34 lbs/gal versus 6.63 lbs/gal), a large outage (using water) was required to keep the theoretical gross rail load of the trucked car to its maximum rating of 286,000 lbs. This was calculated using a 2 percent typical outage for crude oil.

Holes were cut in the bolster flanges of the test article cars and a section of steel round stock welded in the hole centered about the flange. These tubes act as the pivot when engaged in the bearing provision in the tank support fixture. An additional reinforcing structure was added, connecting the round bar to the tank and bolster flange. This was necessary to alleviate high bearing stresses in the bolster flange as the tank pivoted its full weight on the bearings. The taut wire method was used to insure adequate alignment between the bars at each bolster.

Figure 2-1. FRA Test Article

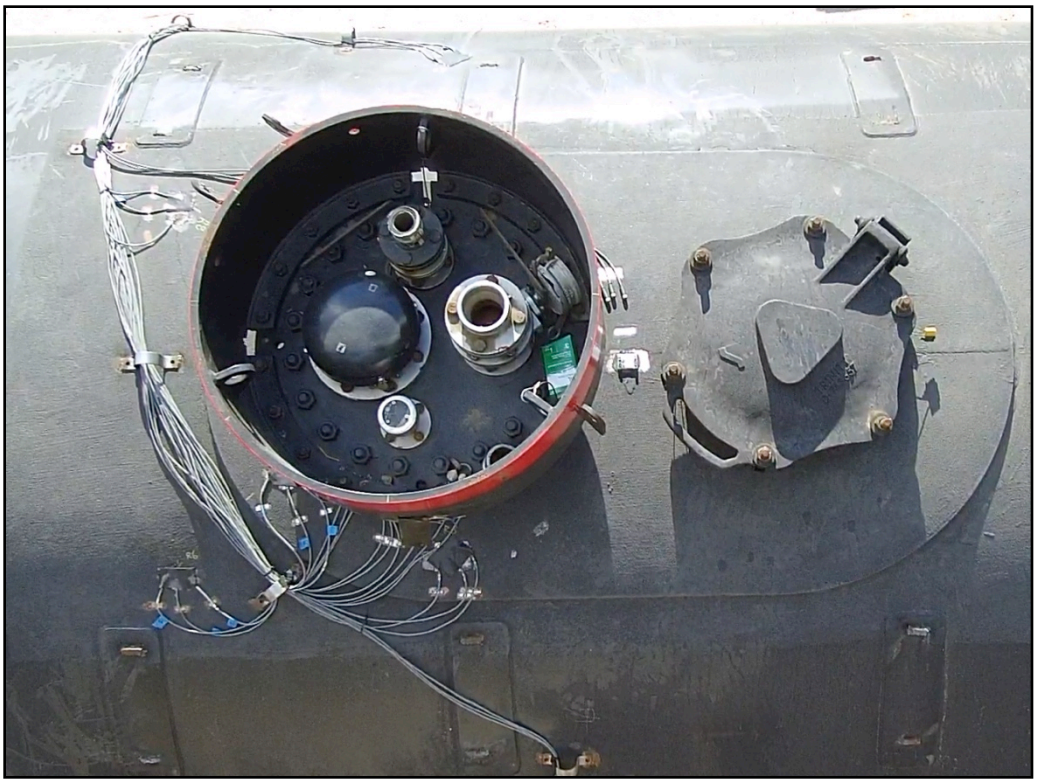

Figure 2-2. Top Fittings – FRA Test Article Close-Up

Figure 2-3. Top Fittings – FRA Test Article

3. Test Description

The full-scale tank car was placed into a test fixture designed to roll the entire loaded un-trucked carbody about a fixed pivot. The tank was filled with water to a 20 percent outage. The carbody was pushed to the point of imminent rotation and then rotated under the force of gravity until impact. A concrete surface target was used to stop the car rotation and provide for impact of the top fittings manway bonnet. This type of arrangement was chosen to control the impact of the top fittings with the target surface and provide repeatable test conditions. An additional advantage of this arrangement was that the vertical location of the concrete target surface was adjustable – to obtain different impact speeds as agreed upon by FRA, SA and industry partners. The tank shell, unloading nozzle, and manway bonnet were instrumented with strain gauges and accelerometers to obtain stresses and forces on the materials (Figure 2-3).

High-speed videos were taken of the rollover test to record the event and determine the impact velocity.

A drone with a high-quality camera surveyed the test area after the rollover to assess the immediate damage from a safe distance.

Post-test analysis of the test article was performed to determine deflections, damage to the structure, and compromises to tank integrity.

The impact of the unloading nozzle bonnet, the highest profile component, was selected to be the focus of the test. The concrete target block was elevated sufficiently to produce the desired impact speed. The underlying block was placed to produce an impact angle of about 77° between the fittings and the target surface (Figure 3-1) and to maintain consistency with previous rollover tests.

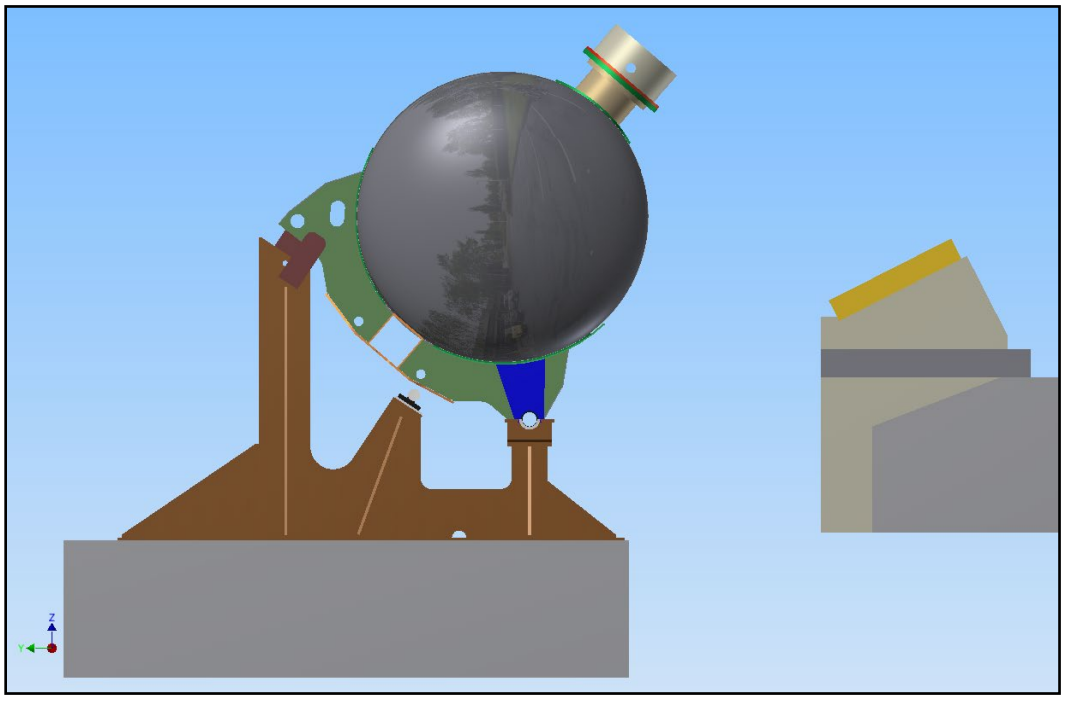

(a) Initial position

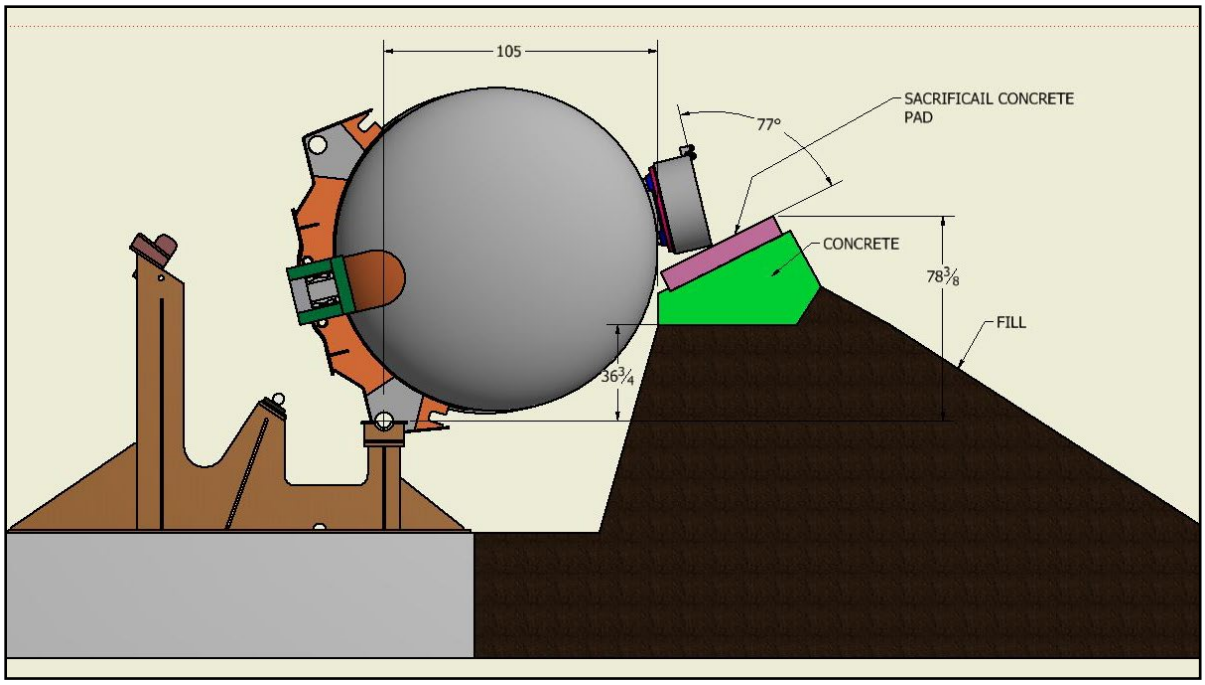

(b) Impact Position

Figure 3-1. CPC-1232 Car Test Layout

Figure 3-2. FRA Tank Carbody in Test Fixture

4. Test Apparatus

The test apparatus consisted of:

- Two fabricated tank support fixtures
- A concrete support base
- A concrete target area
- A hydraulic system
- Instrumentation

4.1 Test Fixture

Two fabricated fixtures were used to support the tank car body, one at each bolster. A concrete base was poured at each fixture location to anchor the fixtures – large enough to accommodate a range of tank car sizes for future testing. Plain pivot bearings were provided integral with the fixtures to accept a shaft that was welded perpendicular to each carbody bolster web. These bearings are made from steel tube stock and have a lower and upper half. After the shaft was placed in the lower half bearing, the upper half bearing was bolted to secure the tank body in position in the fixture (Figure 4-1 and Figure 4-2).

A 75-ton hydraulic cylinder was mounted in each fixture with a clevis eye and roller attached (Figure 4-3). The roller exerts force on the bolster flange to roll the tank car body about the pivot bearing.

4.2 Hydraulic System

The hydraulic system consisted of the following components:

- (1) Electric induction pump, 20L
- (2) 75-ton double-acting cylinders
- (3) 2½” gauge, 0–10,000 psi
- (4) Appropriate high-pressure piping, including valves, hoses, couplers, etc.

The single pump powered both cylinders through a setup of manifolds and valves. The symmetry of mass of the tank car body test articles provided for uniform cylinder extension speed.

Figure 4-1. Bearing to Accept Pivot Shaft

Figure 4-2. Pivot Shaft

Figure 4-3. Hydraulic Cylinder and Rollers

4.3 Instrumentation

A dynamic FEA analysis was performed in order to select appropriate locations for the mounting of strain gauges. Locations close to the areas of interest near or on the fittings or protective structure and far enough away from steep strain gradients were selected. Several locations on the tank shell were also instrumented with strain gauges to determine stresses at these locations and to obtain data to compare to simulations. The bondable gauges were able to record up to 200,000 micro-strains. Strain gauges were bonded to the test specimen surfaces using an automatic strain gauge bonding system. A total of 8 rosettes and 1 single grid gauge were employed (Figure 4-4 through Figure 4-7) with a Somat eDAQ-lite data collection system to collect data for the 28 channels.

An accelerometer was mounted on the tank shell adjacent to the manway to record forces experienced during impact.

A ribbon switch was installed on the target to provide a pulse to record the time of impact.

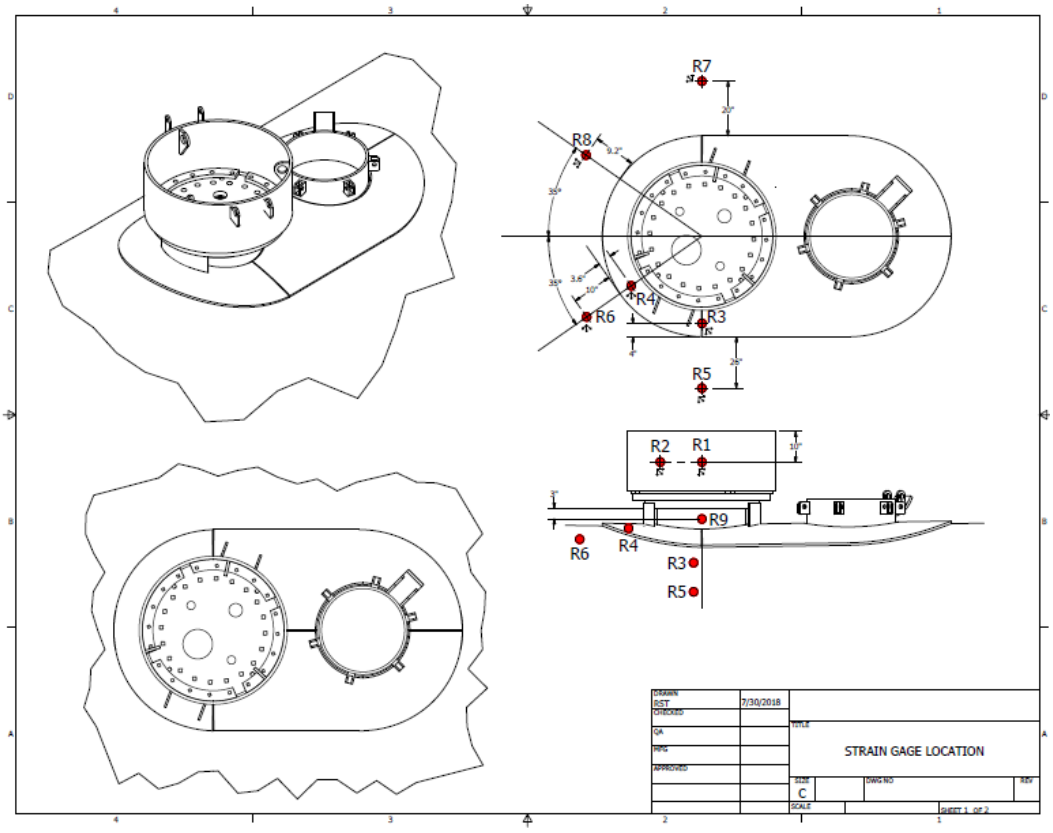

Figure 4-4. Strain Gauge Instrumentation – (R=rosette, S=single gauge)

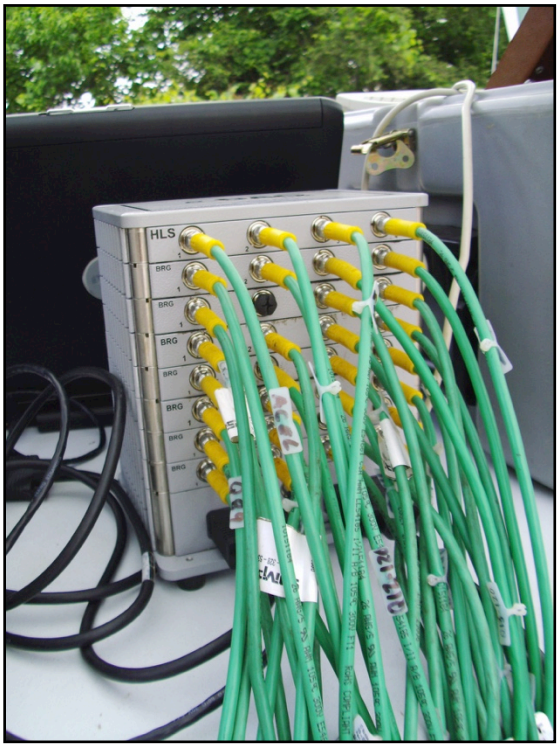

Figure 4-5. Somat eDAQ-lite Data Acquisition System

Figure 4-6. Strain Gauges Being Bonded onto Tank Shell

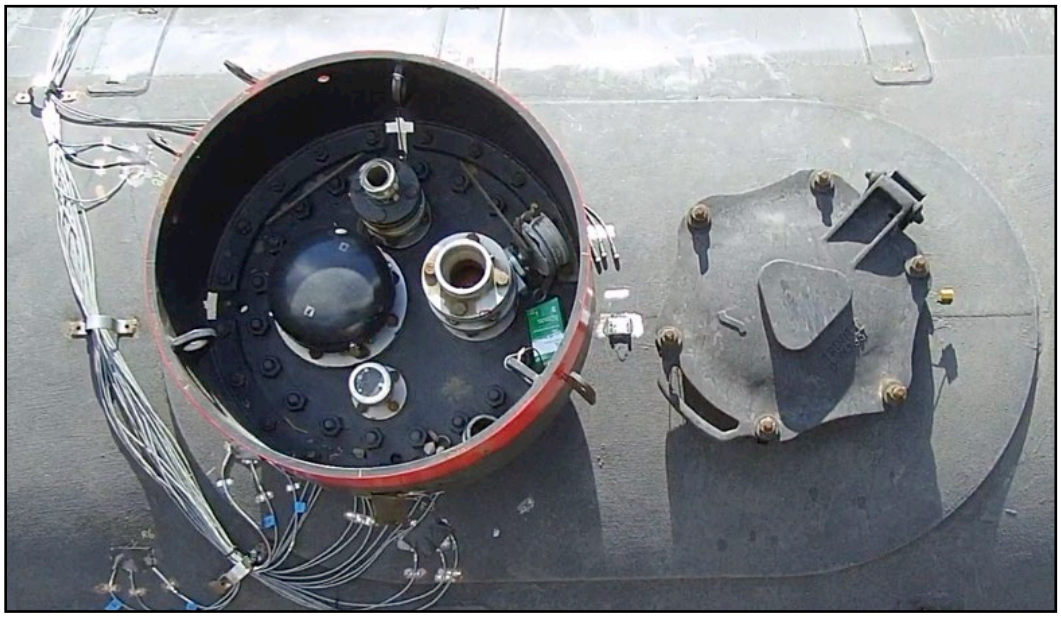

Figure 4-7. Instrumentation on Tank Car Body Test Article

Two digital high-speed cameras (Camera 1 and 2) were used at 3,000 frames/sec to capture the impact of the fittings against the concrete target. Standard digital movie cameras were also captured the overall image and a close-up of the test and impact area (Camera 3, 4, and 5). An aerial drone recorded video of the test site immediately after the rollover.

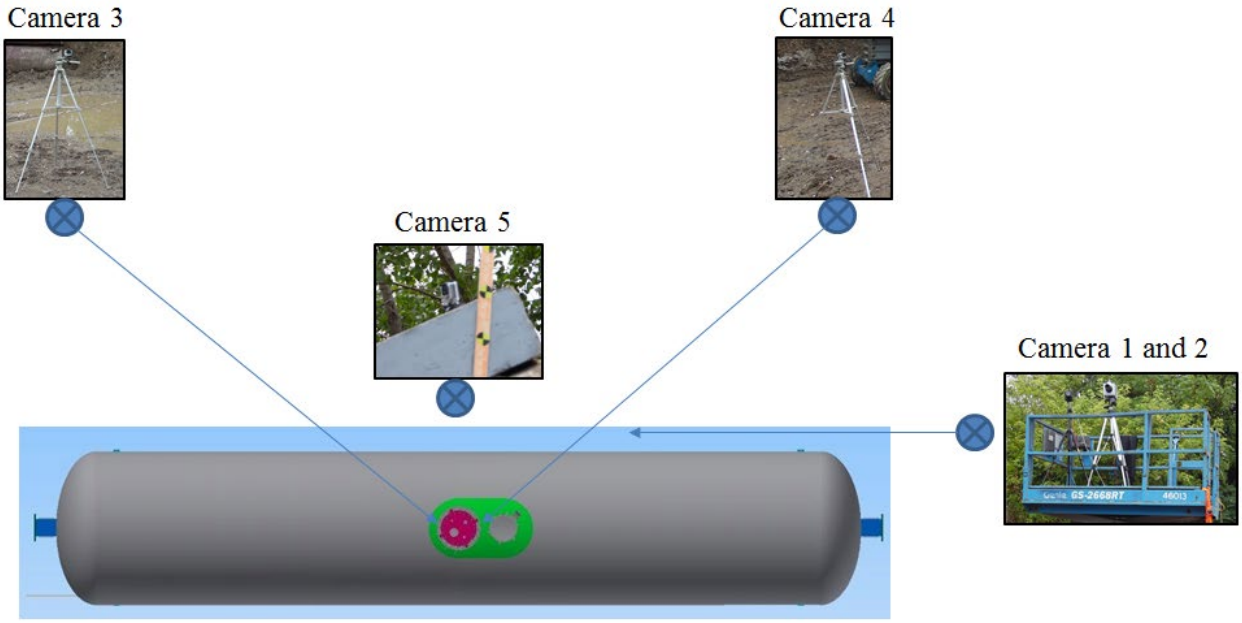

Figure 4-8. Camera Locations

5. Test Results

The initial impact occurred between the leading edge of the manway bonnet and the top sacrificial concrete block. The bonnet leading edge impacted the concrete block at 7.8 mph impact speed. The manway bonnet deformed to where its lateral outside diameter (OD) became 28⅞" and its longitudinal OD became 39⅝". The flange of the leading side of the bonnet deformed in and sheared off the vacuum relief valve causing leaking of water through the connection. All the ¾" studs securing the bonnet to the pressure plate cover sheared off. The bonnet separated from the remaining fittings. Four of the 1⅛" studs fastening the pressure plate cover to the nozzle flange sheared off as the nozzle and cover broke through the top sacrificial concrete block and penetrated a couple inches into the larger block below (Figure 5-1).

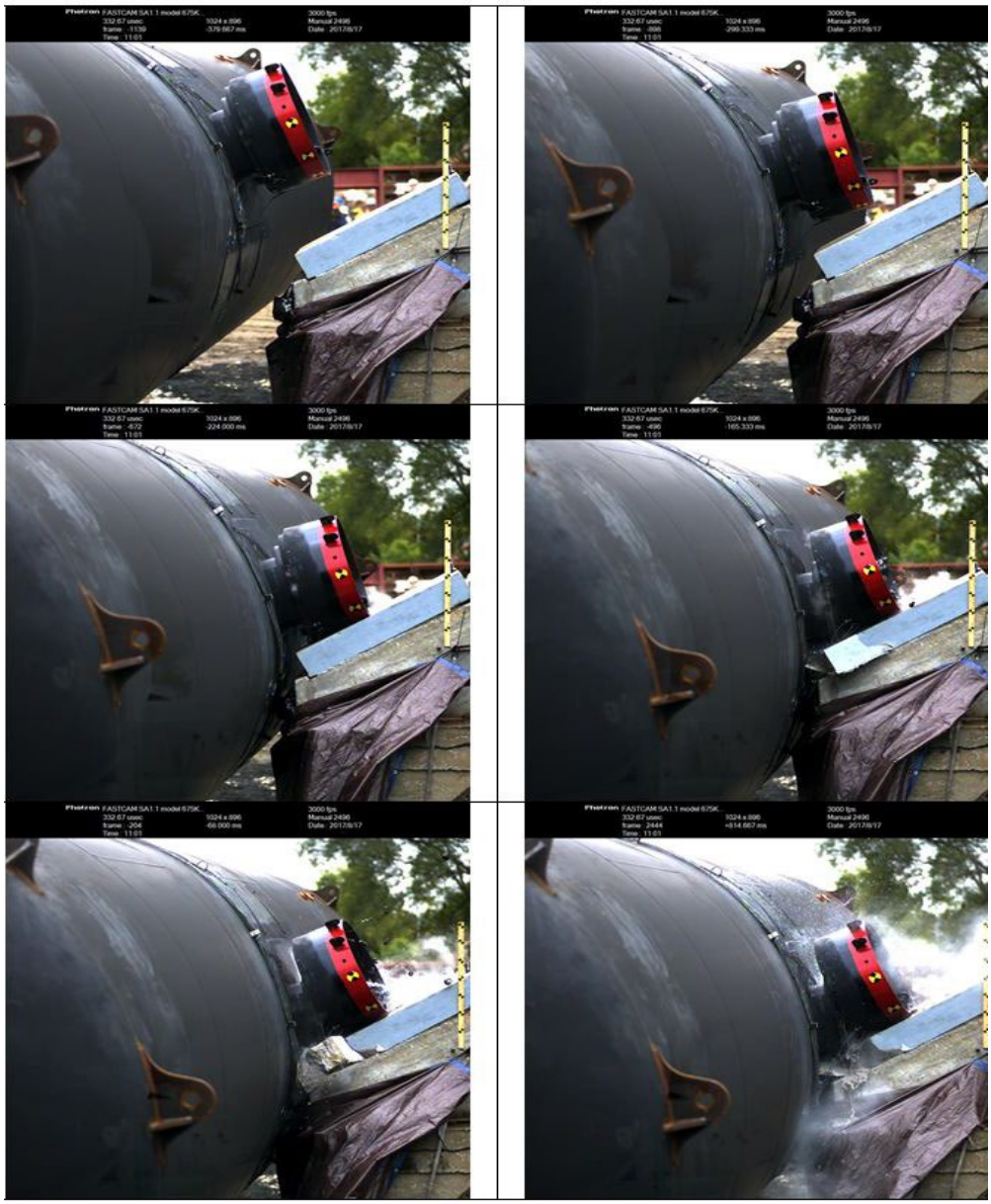

Figure 5-1. Views from High-Speed Camera

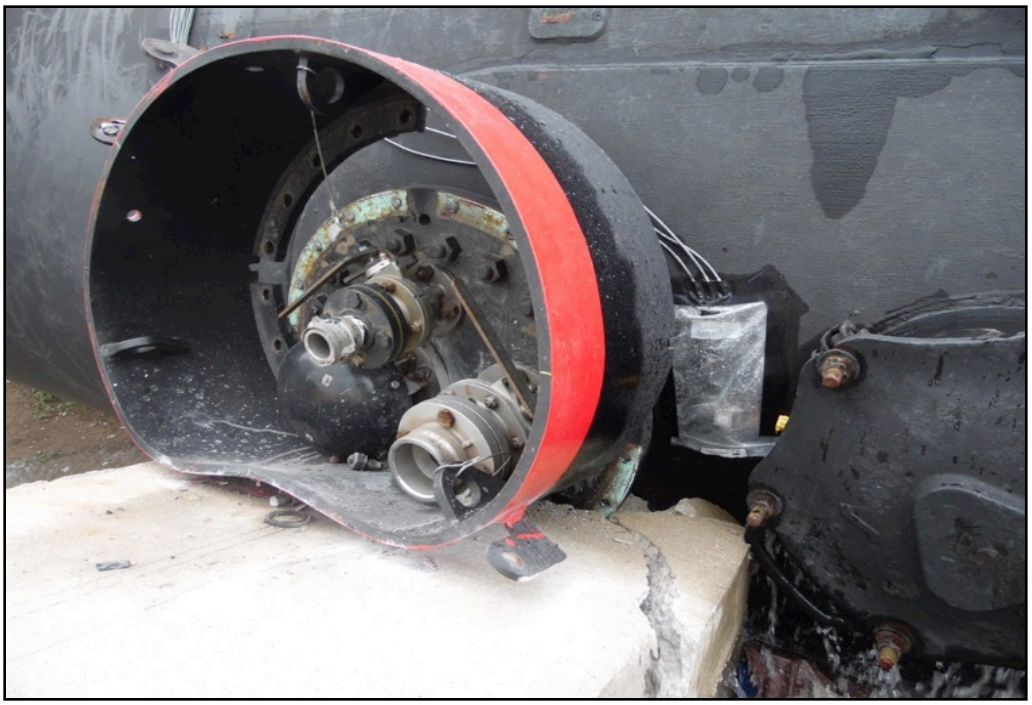

Figure 5-2. Post-Test View 1

Figure 5-3. Post-Test View 2

Figure 5-4. Post-Test View 3

6. FEA Modeling

An FE model was built in a HyperMesh pre-processor from a SOLIDWORKS-based CAD geometry. Mid-surfaces were derived from the solid geometry and stitched appropriately to form the surface geometry for the FE mesh. The surface was then meshed using quadrilateral elements, with a global size of 3.79” throughout the carbody. A refined mesh with a size of 0.5” was used for the top fittings and the concrete, where large deformations were expected in the rollover analysis and regions of high-stress concentrations. The full carbody is shown in Figure 6-1. Details of the top fittings are shown in Figure 6-2. Analyses used LS-DYNA 3D software prior to performing the actual tests. The models were used to first determine the impact speed of the tank car hitting the concrete block and then for the validation purposes.

The tank car shell was modeled primarily with Belytschko-Tsay shell elements. This type of element is computationally efficient in LS-DYNA and is a widely used shell element formulation for crash and impact applications. The top fittings and the concrete blocks are modeled with 8-node solid hexahedron elements, also called fully integrated S/R solid. The full integration elements were used in the analysis to control the hourglass energy.

The tank car body was pinned in a fixture and allowed to rotate about the longitudinal axes. There was no initial velocity. The tank was subjected to the gravity force and accelerated under gravity until impact similar to the test conditions.

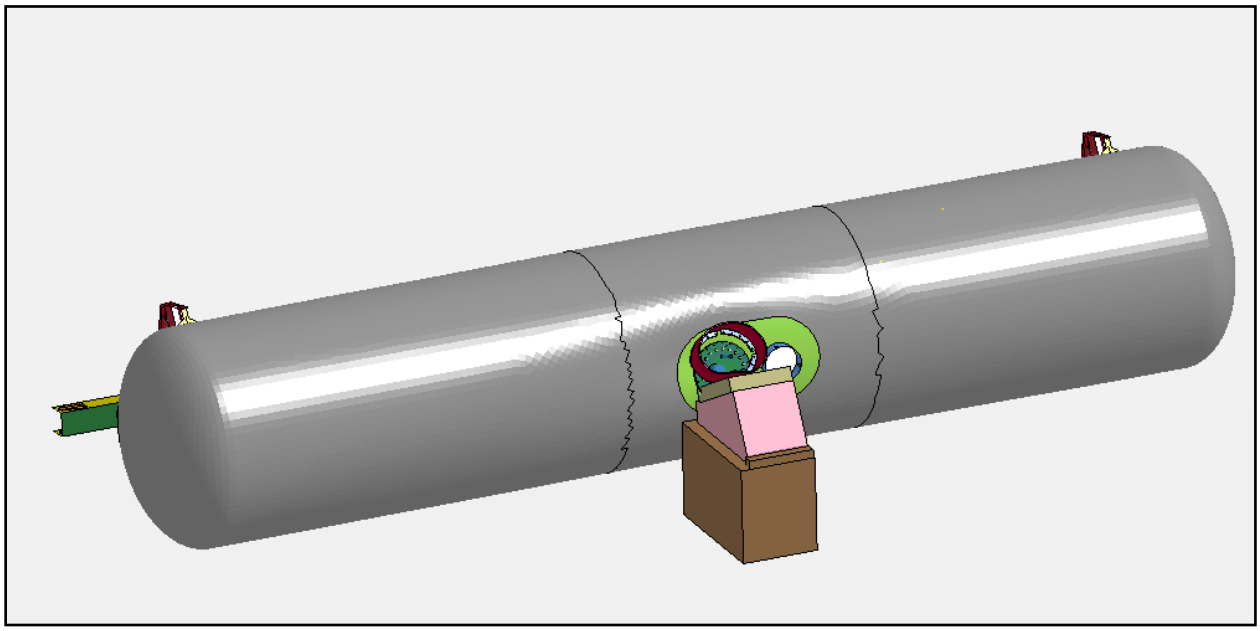

Figure 6-1. FE Model – LS-DYNA

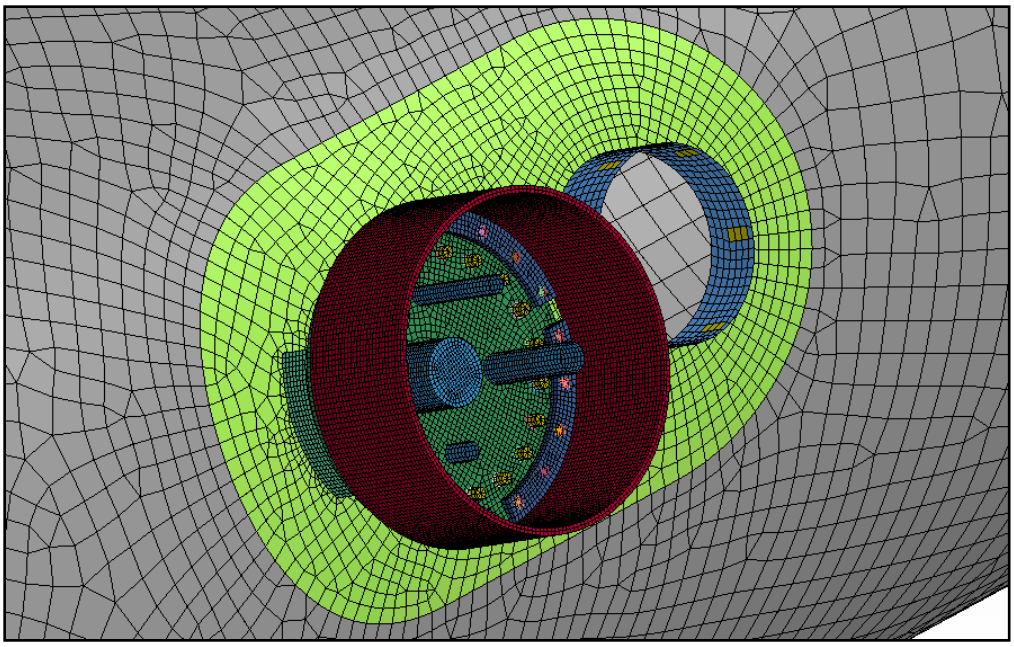

Figure 6-2. Mesh Details of the Top Fittings

Each stud on the top fittings was modeled using two-node spot weld beam elements. The spot weld beam elements (ELFORM = 9) were based on the widely used Hughes-Liu beam formulation (Figure 6-3). Each beam element was given the appropriate cross-section, diameter, and material properties to represent the actual fastener material. An initial axial force pre-load was placed on each mechanical fastener, consistent with the recommended torque for each stud (61,213 psi for the pressure plate studs and 29,557 psi for the bonnet studs). A proof load of 85 percent of the yield strength was used to determine the studs preload. Originally, both types of studs had the same material properties. Post-test Brinell hardness tests on the bonnet and fittings plate studs found material properties of the pressure plate bolts lower than bonnet bolts (Table 6-1). Stress-based failure criteria were defined only in terms of normal and shear stresses.

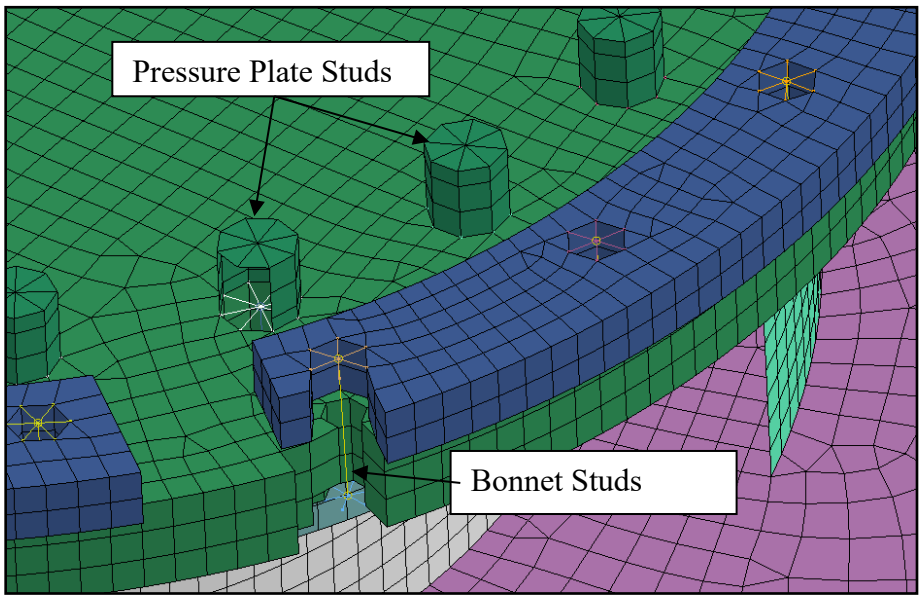

Figure 6-3. Model for the Fittings Plate Studs

Material	Yield Strength (psi)	Tangent Modulus (psi)	Ultimate Strength (psi)	Poisson Ratio
A516 Gr 70 for Top Fittings	38,000	153,846	70,000	0.29
TC-128 (tank car)	50,000	164,894	81,000	0.29
A572 Grade 50 (bolster)	50,000	73,558	65,300	0.29
ASTM A36	36,300	112,719	62,000	0.26
Fittings Plate Bolts	96,600	116,500	115,000	0.3
Bonnet Bolts	115,000	126,582	125,000	0.3

Table 6-1. Material Properties

The failure of the fittings plate bolts in the test seems to have been due to high shear forces seen by the studs when in contact with the bonnet.

6.1 Results – FEA Simulation of FRA Rollover Test

As mentioned previously, pre-test and post-test simulations were performed using LS-DYNA 3D. Sequential images from the simulation are shown in Figure 6-4. The results of the simulation agreed well with the actual test results (Figure 6-5). The tank car body rotated about its pivot under the influence of gravity and impacted the target at 7.8 mph (Figure 6-6). The bonnet leading edge deformed in by 6.9” in the simulation. The bonnet itself then broke away as its attaching studs failed. The remaining portion of the fittings assembly simultaneously pushed the concrete target angled block and sacrificial block outward and broke through some of the leading edge of these blocks. It then proceeded to break into the next underlying block where it finally stopped.

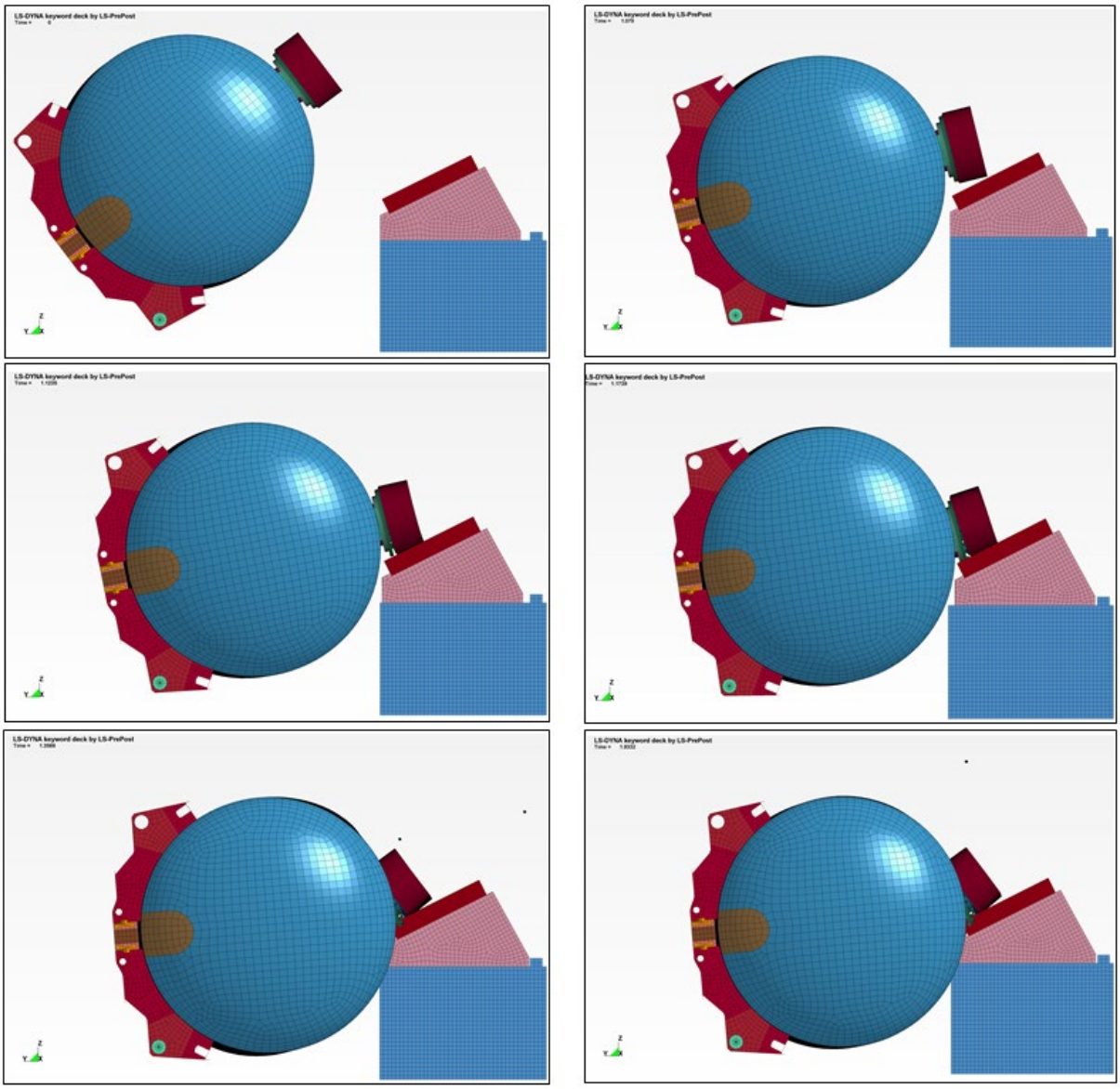

Figure 6-4. Sequential Images from Simulation

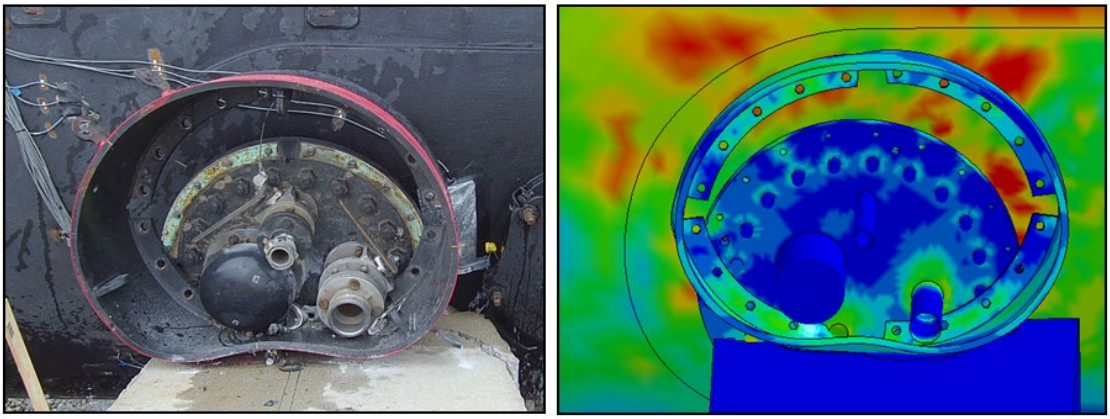

Figure 6-5. Comparison between Test and FE Simulation of the Bonnet Deformation

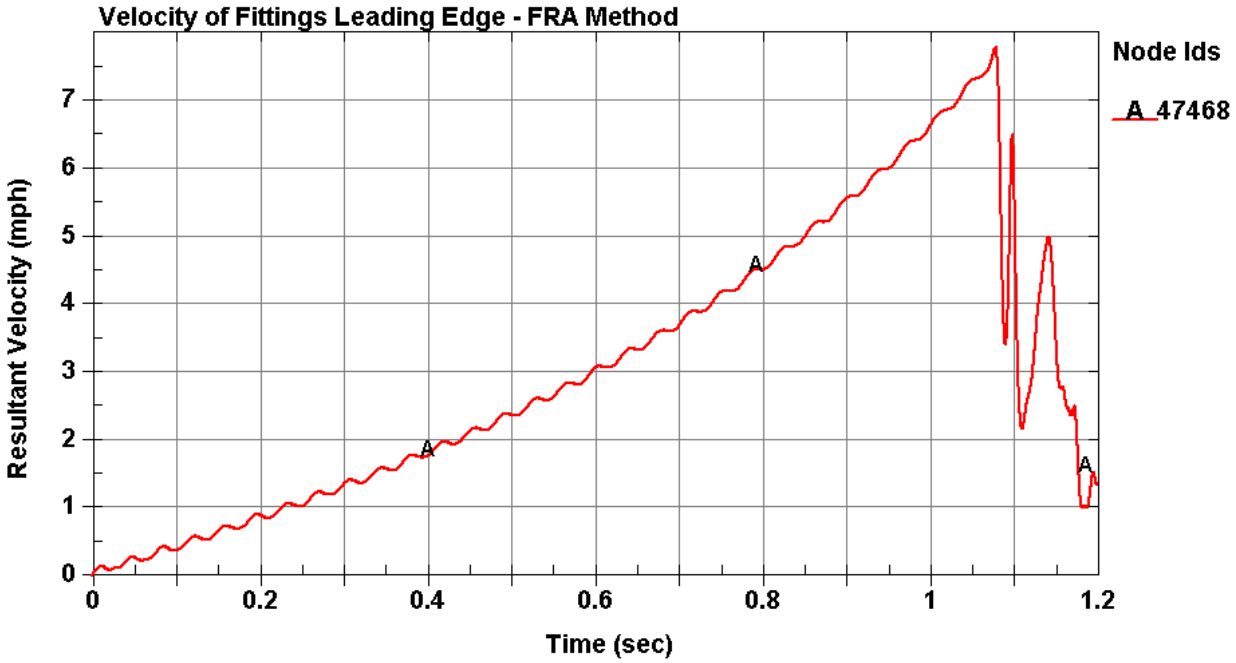

Figure 6-6. Velocity of Bonnet Leading Edge

Figure 6-7 shows a 3D von Mises stress contour plot of the bonnet deformed on the sacrificial block prior to its separation from the remaining fittings. A comparison of the deformation of the bonnet's leading edge between the simulation and the actual test is shown in Figure 6-8. Final deformation of the bonnet in the test was similar to the FE simulation.

The effect of the bonnet and fittings cover plate breaking through the concrete material can clearly be seen in Figure 6-9. The bonnet had already separated and the fittings were crushing into the second layer of concrete. The test and simulation were predicting same number of failed studs on both the bonnet plate and fittings plate. However, the number of fittings plate studs that failed in the simulation had a different pattern than the test – almost a mirror image of the test. This could have been because of the simplified geometry of the valves fittings in the FE model.

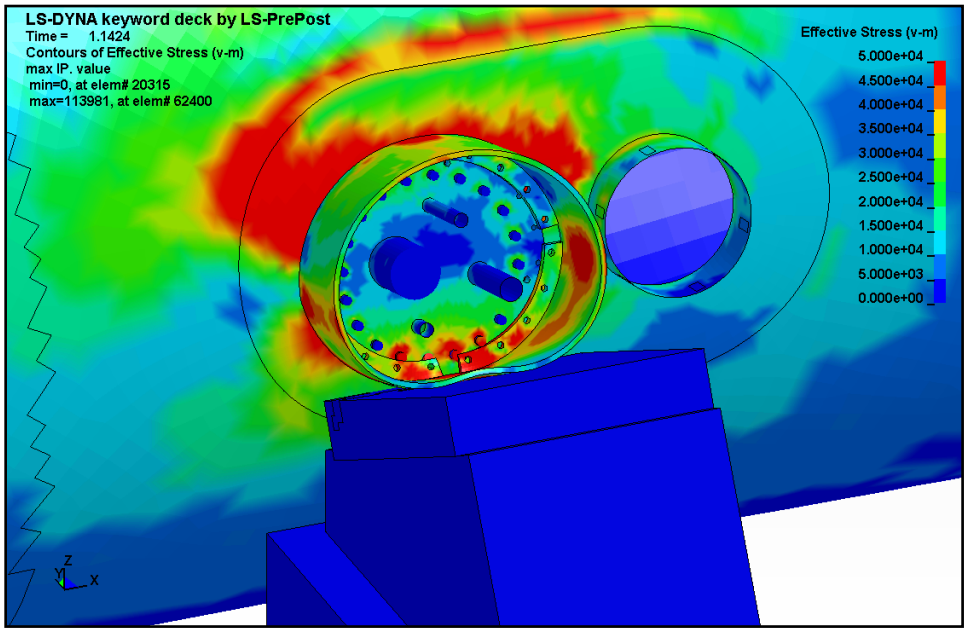

Figure 6-7. von Mises Stress Contour Plot of Fittings Impacting Target

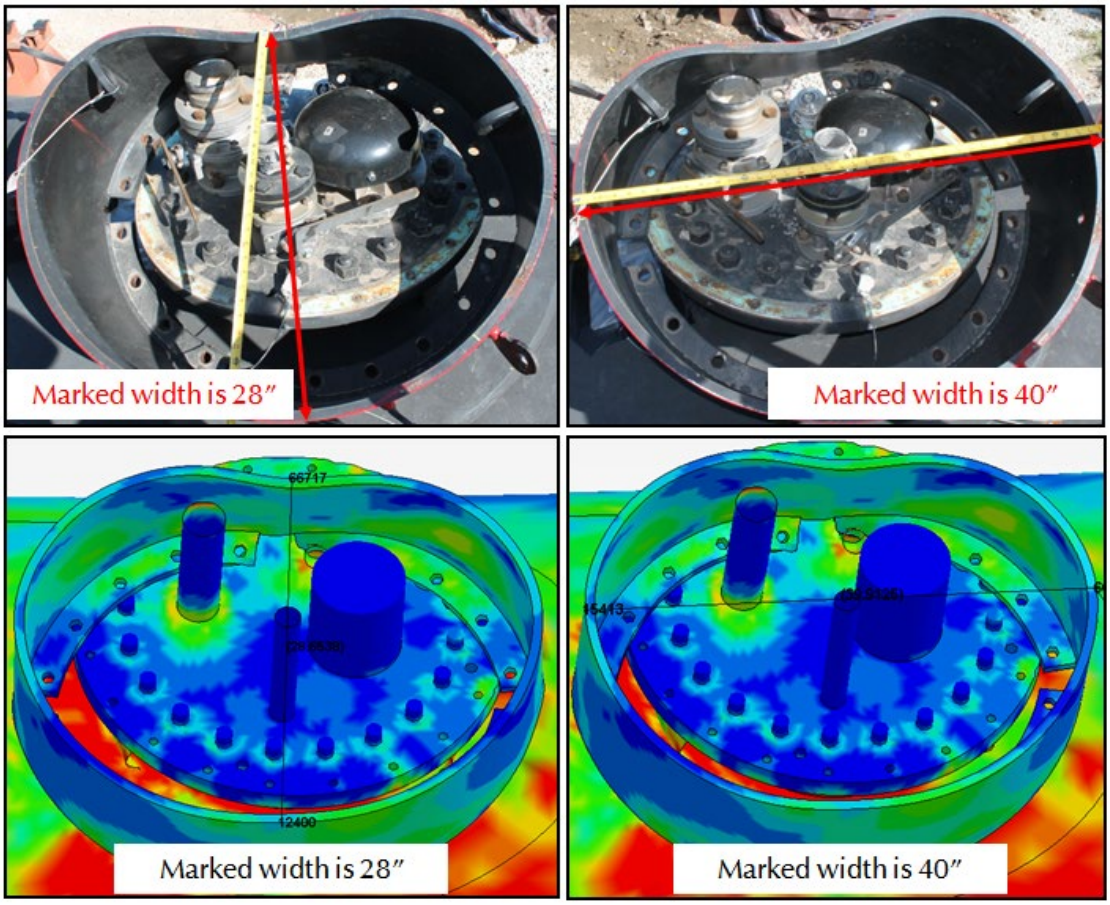

Figure 6-8. Bonnet Deflection – Test vs. LS-DYNA

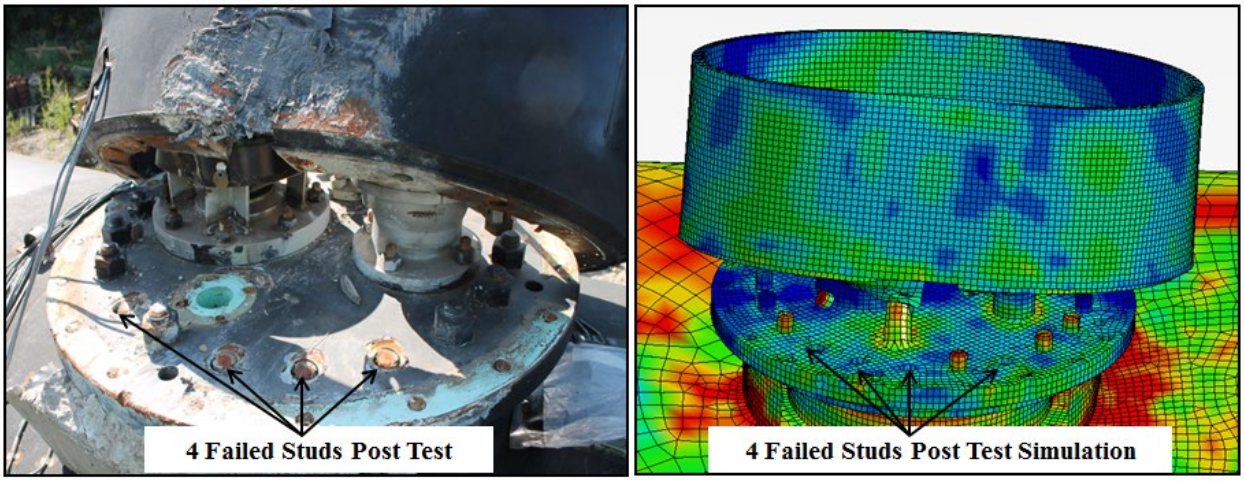

Figure 6-9. Correlation between Test and LS-DYNA

The force between the bonnet and the fittings is plotted in Figure 6-10. The force reached 988,000 lbf during the duration of the bonnet detaching from the fittings plate. The lower 8 bonnet studs (¾" diameter) failed almost simultaneously, followed by the next 12 studs (¾" diameter) that failed in sequence.

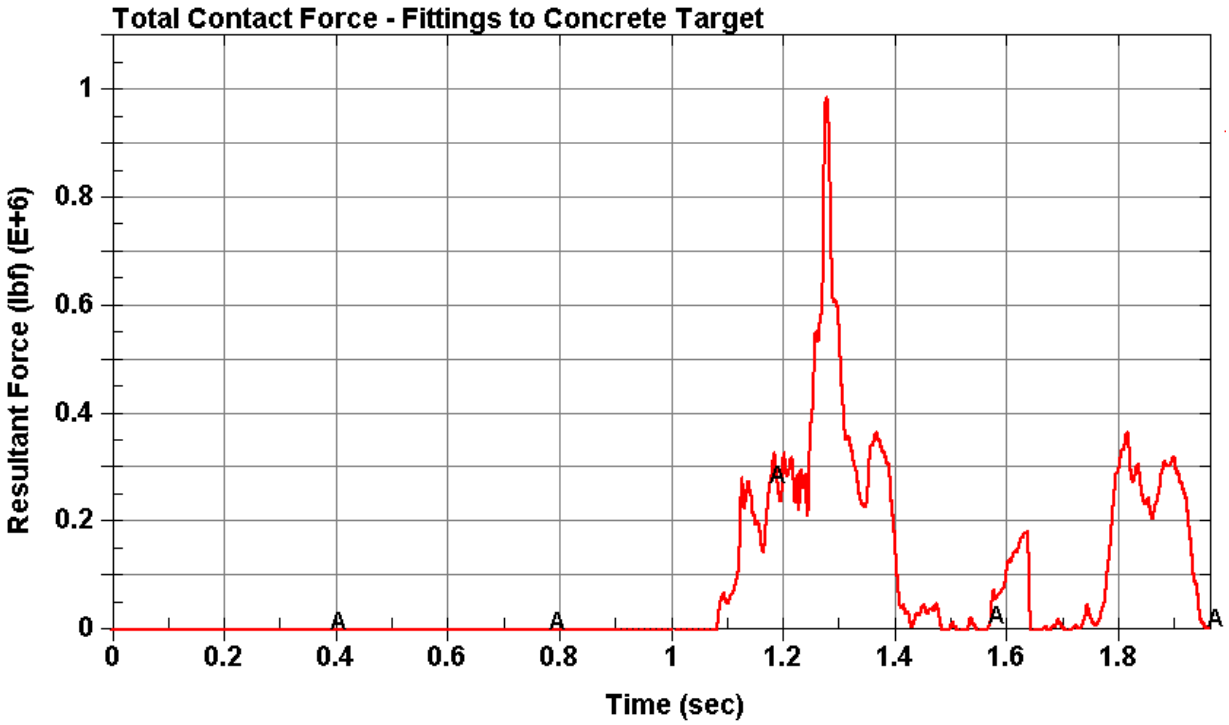

Figure 6-10. Total Contact Force – Fittings to Concrete Target

Figure 6-11 shows the resultant forces of the first eight failing studs. The plot shows the beam elements were preloaded to 29,557 lbf for bonnet bolts and 61,213 lbf for the fitting plate studs. The preload was calculated based on the section area of the stud, the proof load (85 percent of the yield stress), and stud coefficient of 0.75 (for connections requiring reuse).

The calculated axial failure force for the ¾" diameter bolts was 37,750lbf (area*ultimate stress) while for the 1⅛" diameter bolts it was 72,680 lbf. The shear failure forces were obtained by multiplying the 0.6 factor to the axial failure force. Researchers noticed that all the bonnet bolts were failing too fast (axial failure) with respect to the test, so a few other trials were made to match the simulation with the test. The final axial failure force for the bonnet studs used in the simulation was 43,800 lbf and for the pressure plate studs was 79,700 lbf, while the shear failure force remained unchanged for both types of studs (bonnet and pressure plate) which was a 0.6 factor of the axial failure force. Researchers anticipated that a higher failure force would be acceptable for this dynamic test since the failure force formula was based on a static test.

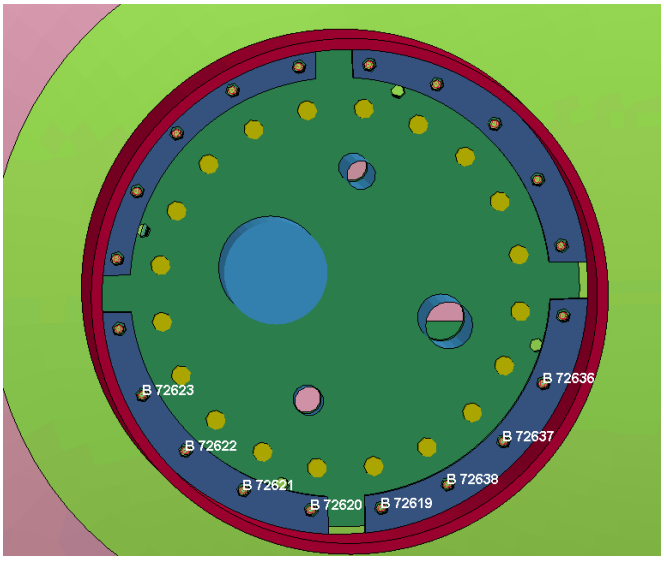

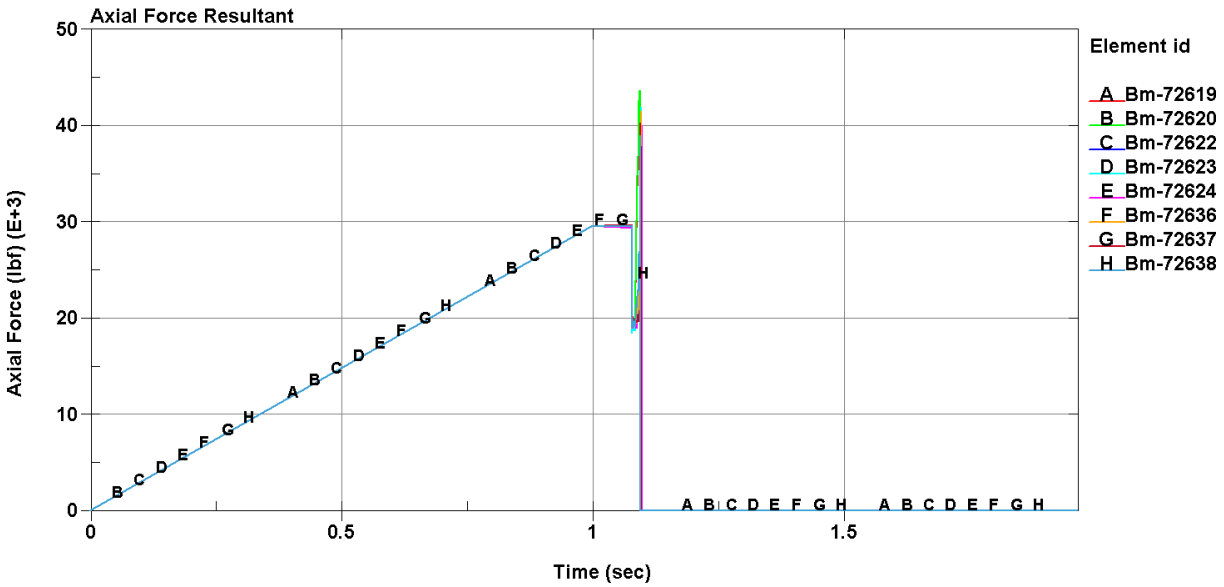

Figure 6-11. Resultant Forces on the First 8 Leading ¾'' Dia. Studs

Figure 6-12 shows a close view of the resultant forces of the failing studs. As expected, the first 2 studs experienced the highest force before failing, followed in sequence by the other 18 studs. Figure 6-13 plots axial and shear forces of the leading bonnet stud #72619. In this plot, shear forces experienced by the studs at the moment of impact were much lower than the axial forces. Figure 6-14 plots axial and shear forces of the leading pressure plate stud #72650. The shear and axial forces of the beam elements that represent the pressure plate studs were all lower than the corresponding failure strengths. This was mainly because of the way the studs were modeled in LS-DYNA, where the beam elements were connecting the two plates, and the nuts were modeled using shell elements. Four nuts (shell elements) in the simulation failed at 0.2 strains, similar with the test results, where four of the pressure plate studs failed because of the shear loads (Figure 6-15).

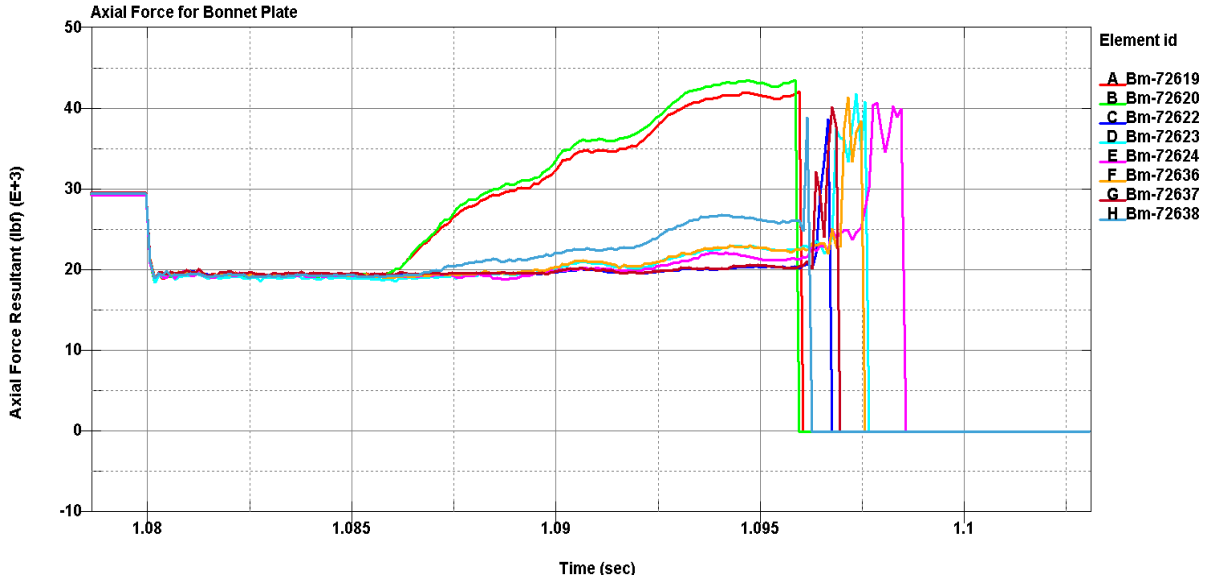

Figure 6-12. Resultant Forces on the First 8 Leading ¾" Dia. Studs (close view)

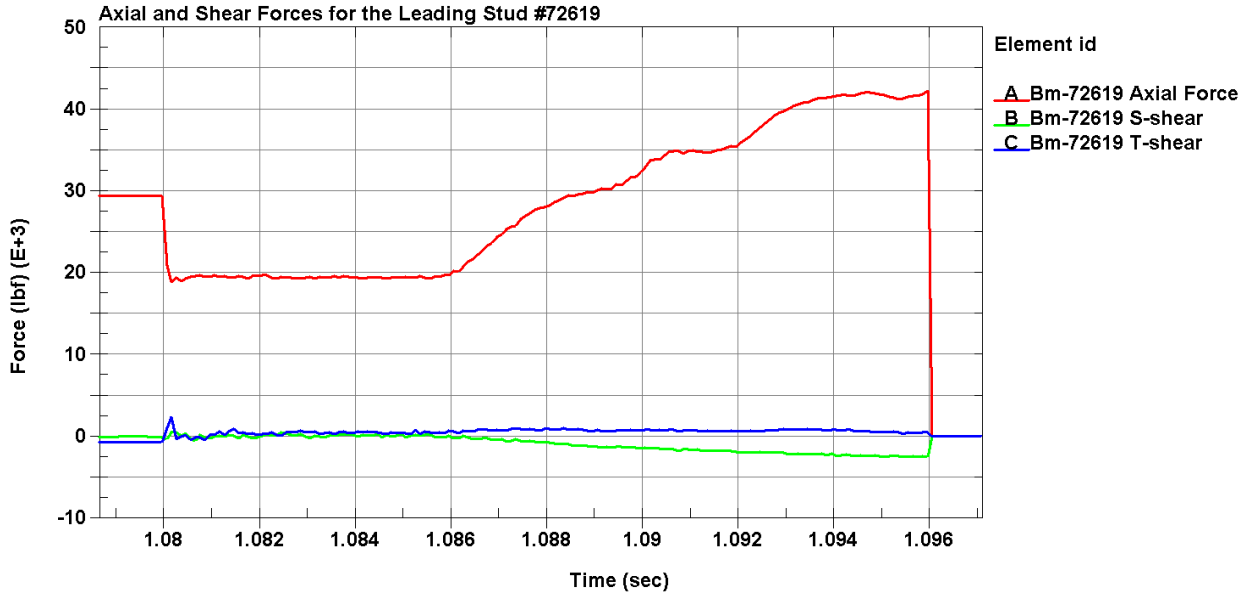

Figure 6-13. Axial and Shear Forces of the Leading ¾" Dia. Stud #72619

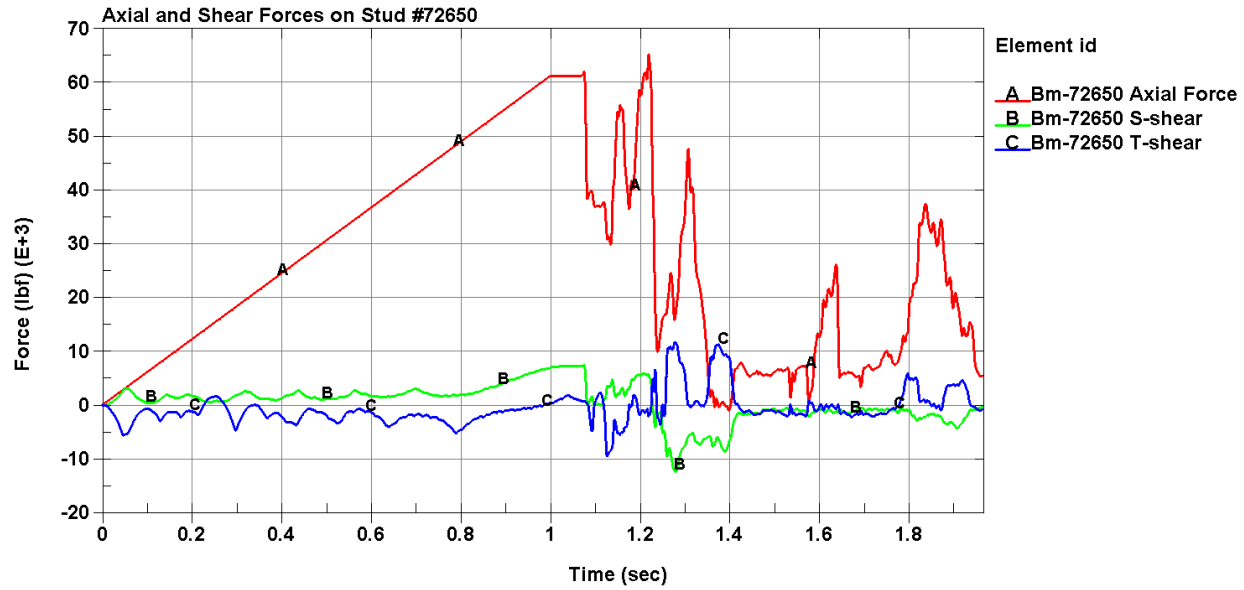

Figure 6-14. Axial and Shear Forces of the Leading 1⅛" Dia. Stud #72650

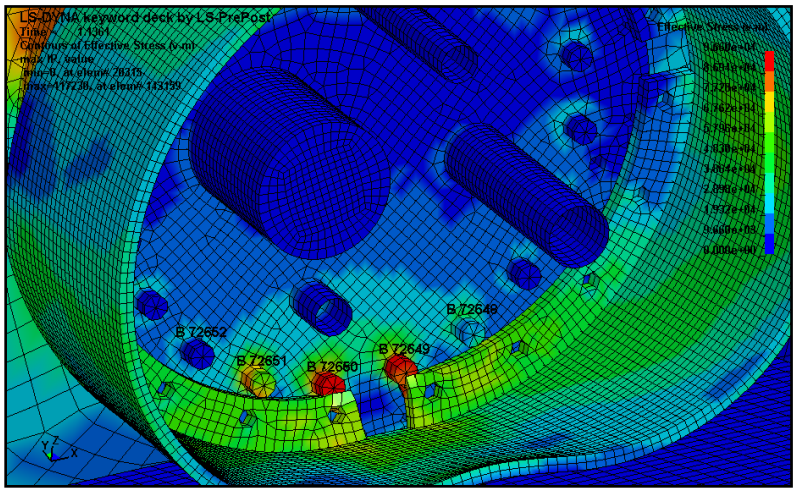

Figure 6-15. Sheared Stud from Fitting Plate

7. Conclusion

Full-scale tank car body rollover testing was successfully performed on a CPC-1232 tank car using the FRA test method to evaluate the survivability of the top fittings in a 7.8 mph impact with a concrete surface. An FEA model was built to predict the appropriate height and location of the target surface and later to compare to the physical test results.

The physical test resulted in the manway bonnet shearing off at its bolted connection, several fasteners securing the pressure plate cover failed, and the unloading/loading valves sheared off. A good correlation was made to the physical test by the FEA simulation, which showed a similar outcome.

A key reason behind the failure seen during the test (and the corresponding simulation) was the sequential failure of bolts observed. The bolted connection between the bonnet and the flange is designed under a static load, which assumes that the bolts are loaded uniformly; however, under actual impact conditions the load distribution is not uniform, with the bolts closest to the point of impact taking the most load. This results in the failure of those bolts, following which, the loads transfer to the next set of bolts, which then fail, leading to an “unzipping” effect and separation of the bonnet from the flange. The research team recommends that the potential for such sequential bolt failure be considered in the design of fittings protection.

8. Recommendations

In this study, the manway bonnet contacted the concrete block at a 7.8 mph impact speed and sheared off at its bolted connections.

The test and the simulations showed that the dominant mode of failure for these designs was the "unzipping" shear failure of both the pressure plate and the bonnet fasteners. The authors recommend that mechanisms to improve the bolted connection be considered. Alternately, one may consider incorporating that failure mechanism into the design and specification process. Additionally, the use of energy absorbing elements in the load path might better distribute the bolt loads resulting in an increased likelihood of survival of the fittings protective structure.

9. References

Federal Railroad Administration, (2006), Survivability of Railroad Tank Car Top Fittings in Rollover Scenario Derailments [DOT/FRA/ORD-06/11]. Washington, DC: U.S. Department of Transportation.

Federal Railroad Administration, (2009), Survivability of Railroad Tank Car Top Fittings in Rollover Scenario Derailments – Phase 2 [DOT/FRA/ORD-09/20]. Washington, DC: U.S. Department of Transportation.

Appendix A.
Sample Test Data

The following images shown in Figures A1 through A6 are sample strain plots obtained in the LS-DYNA simulation compared with those obtained from the strain gauge instrumentation from the actual test. Note that the time scales used in LS-DYNA were different and not comparable to those used with the actual test instrumentation. Figure 4-4 shows the strain gauge locations for the base case.

Output data was filtered using a Butterworth filter at 150 Hz.

A ribbon switch output plot is provided in Figure A7 to indicate the exact time of impact.

Accelerometer plots for both directions in plane with the motion of the tank are shown in Figures A8 and A9. These plots show values of the same order of magnitude and the same general curve shapes between the actual test and those obtained from the simulation.

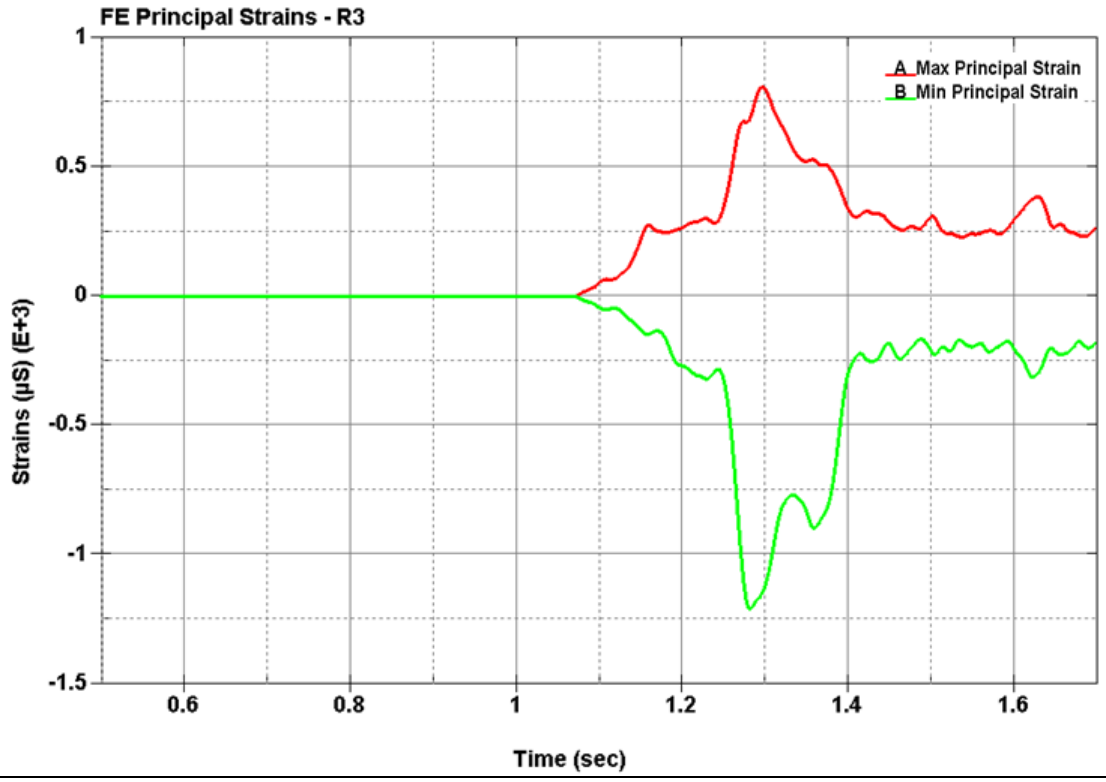

Principle Strains from LS-DYNA Simulation Location R3

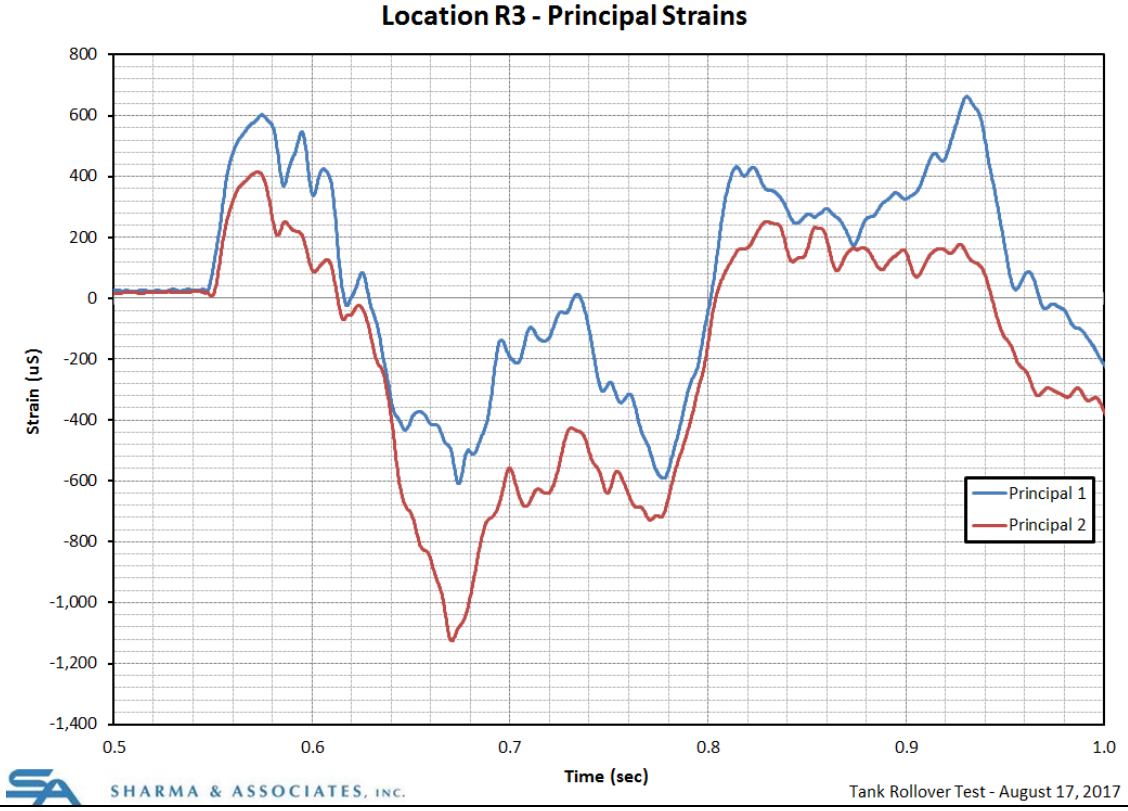

Principle Strains from Actual Test Location R3

Figure A1

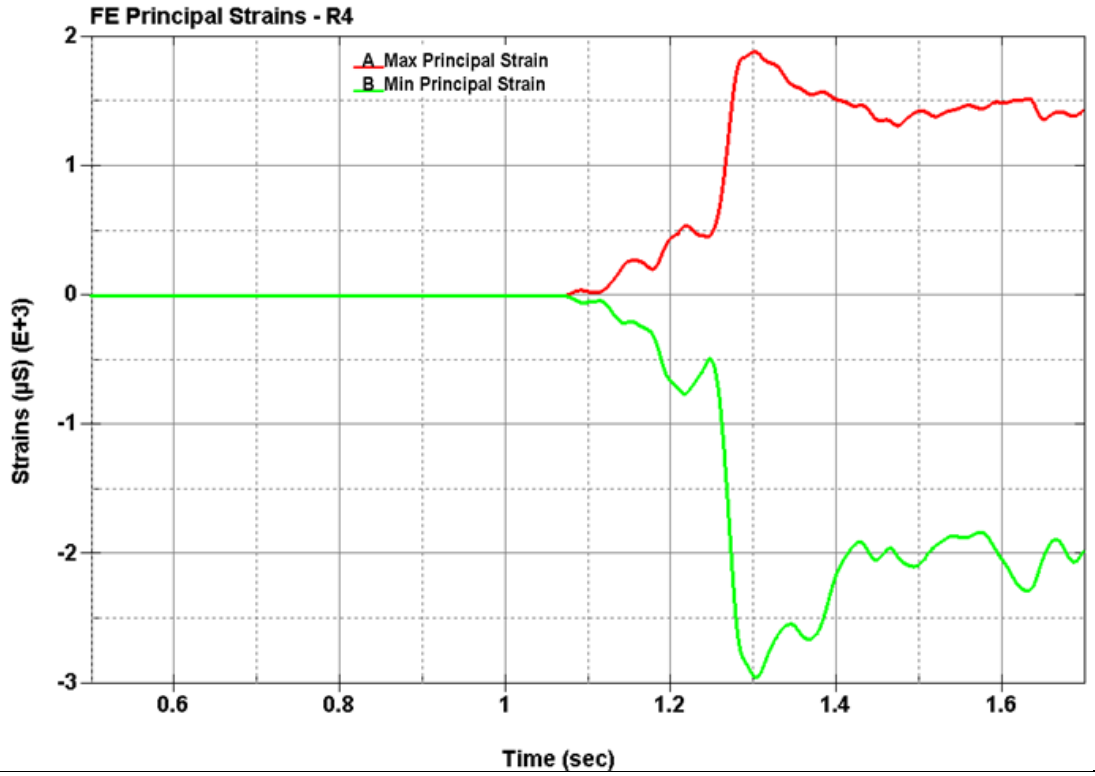

Principle Strains from LS-DYNA Simulation Location R4

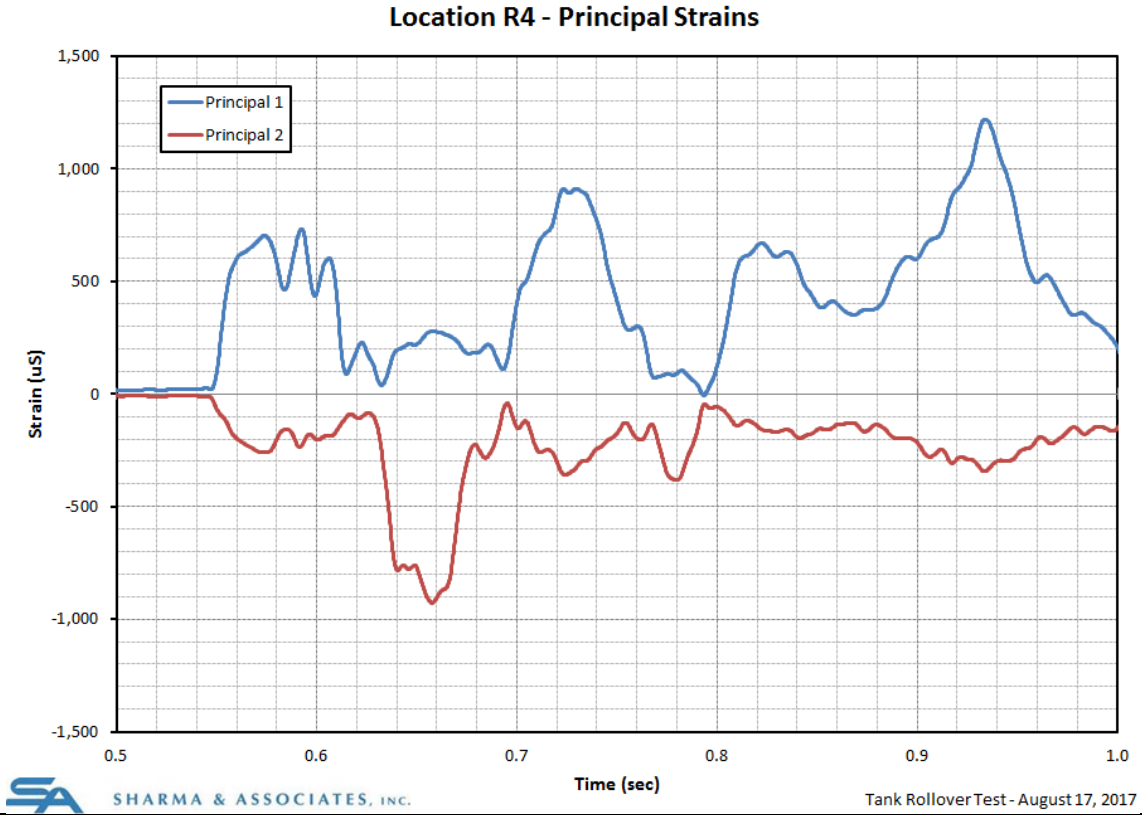

Principle Strains from Actual Test Location R4

Figure A2

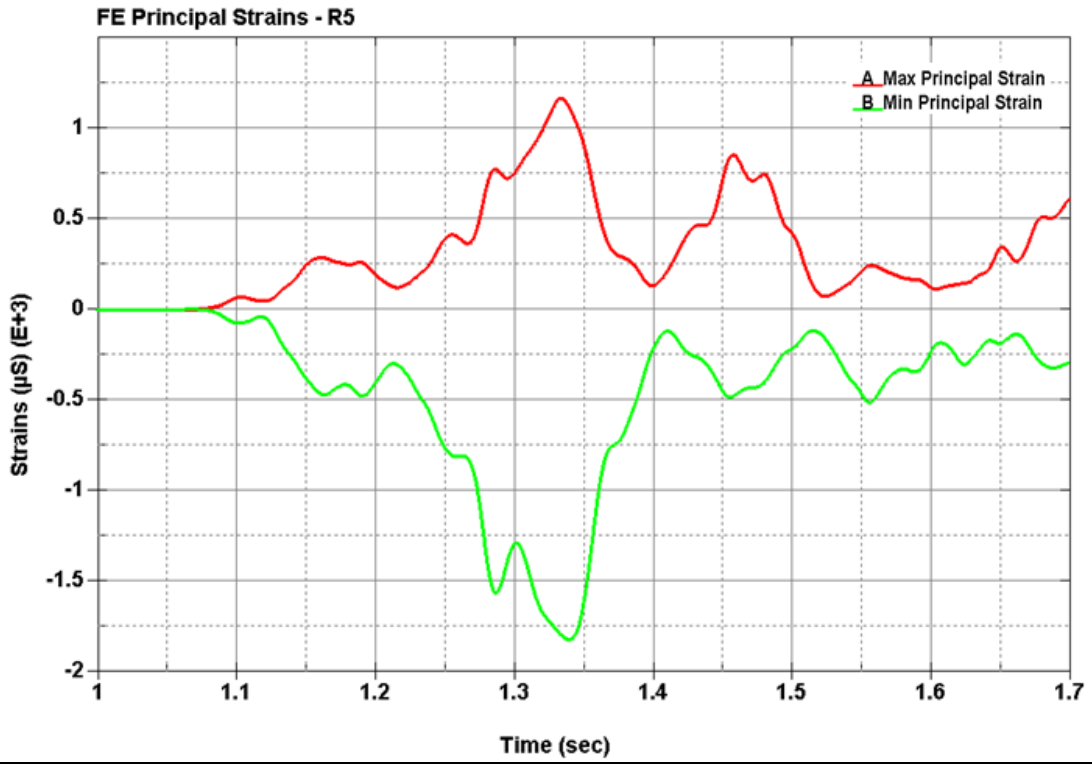

Principle Strains from LS-DYNA Simulation Location R5

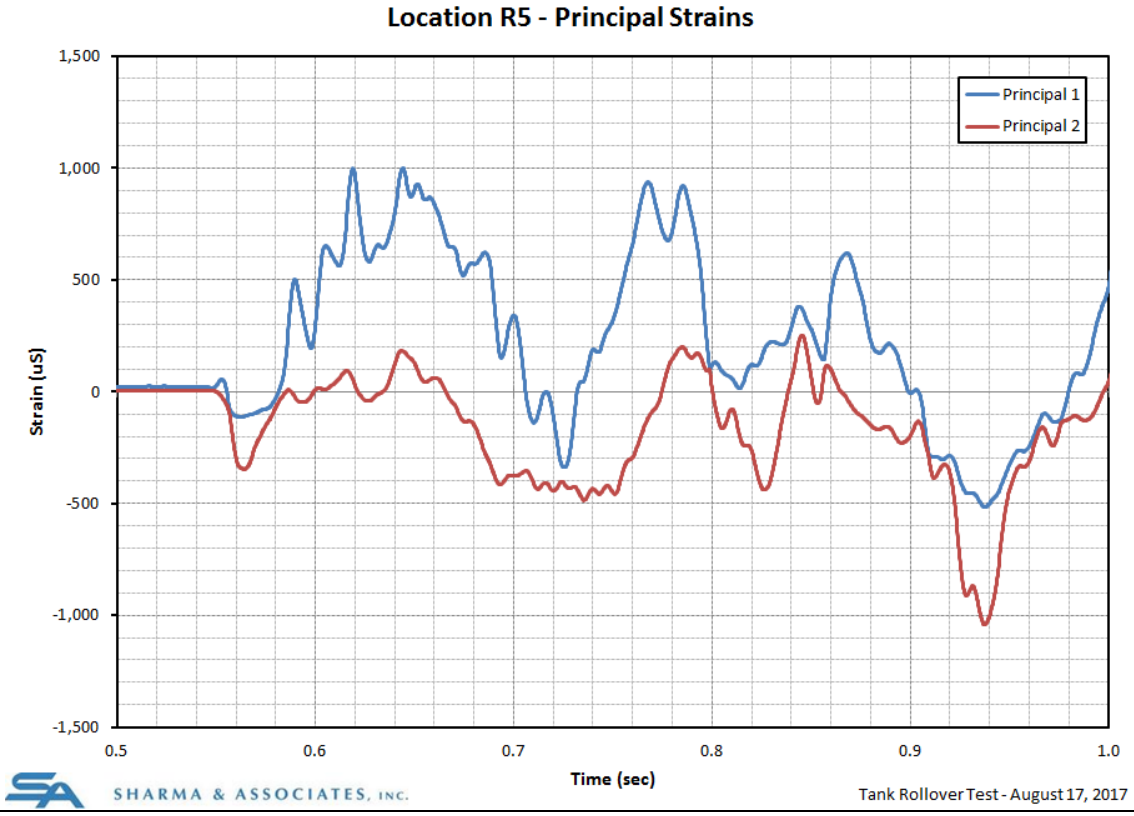

Principle Strains from Actual Test Location R5

Figure A3

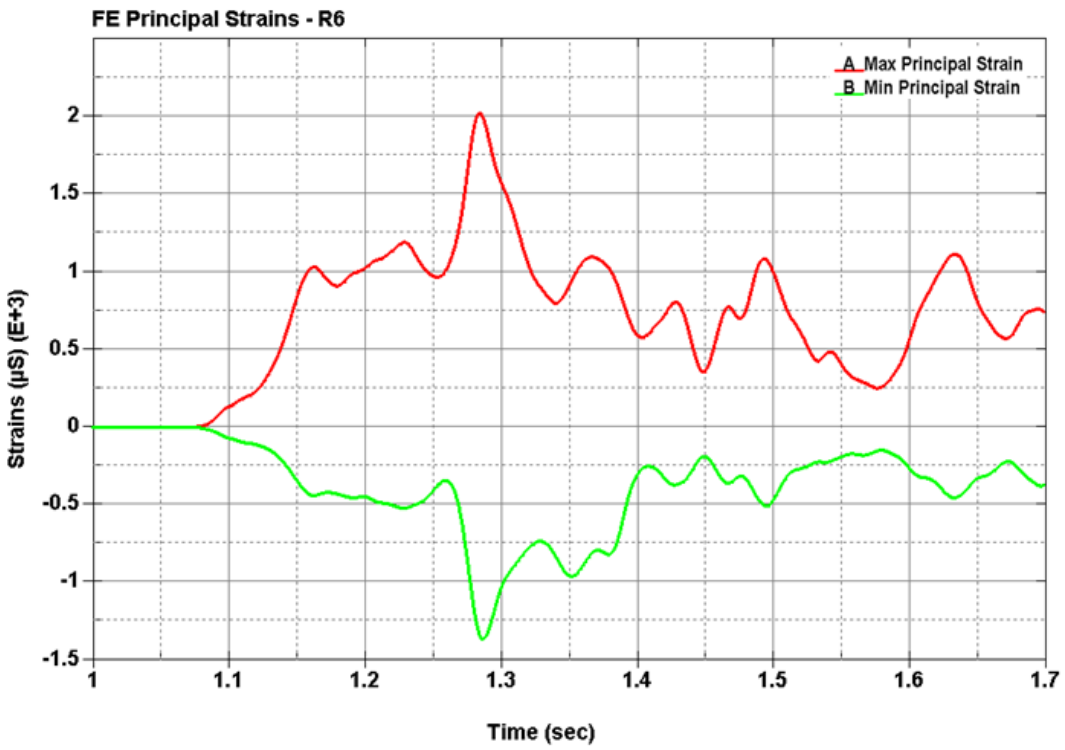

Principle Strains from LS-DYNA Simulation Location R6

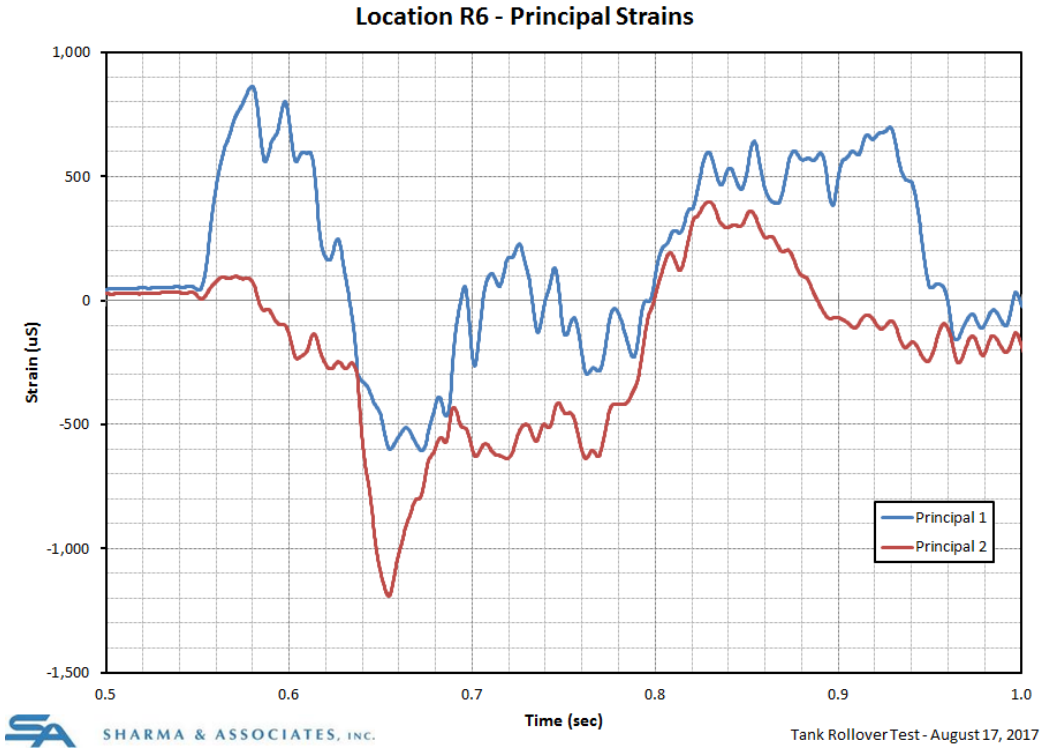

Principle Strains from Actual Test Location R6

Figure A4

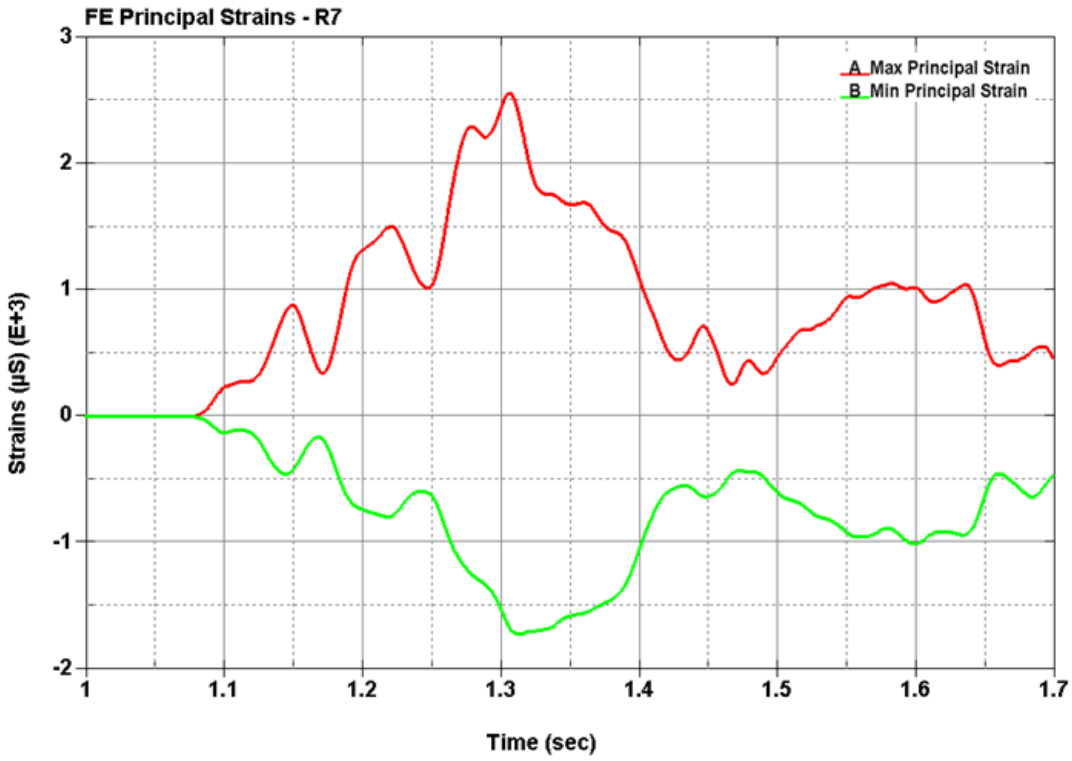

Principle Strains from LS-DYNA Simulation Location R7

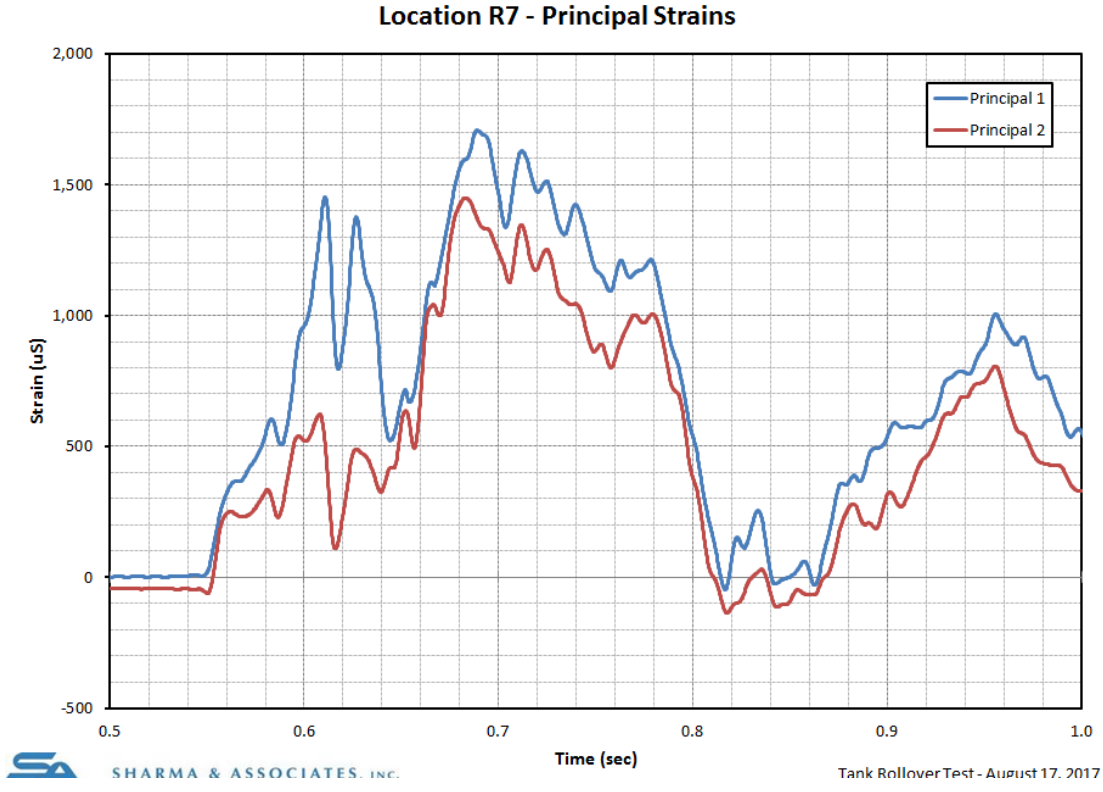

Principle Strains from Actual Test Location R7

Figure A5

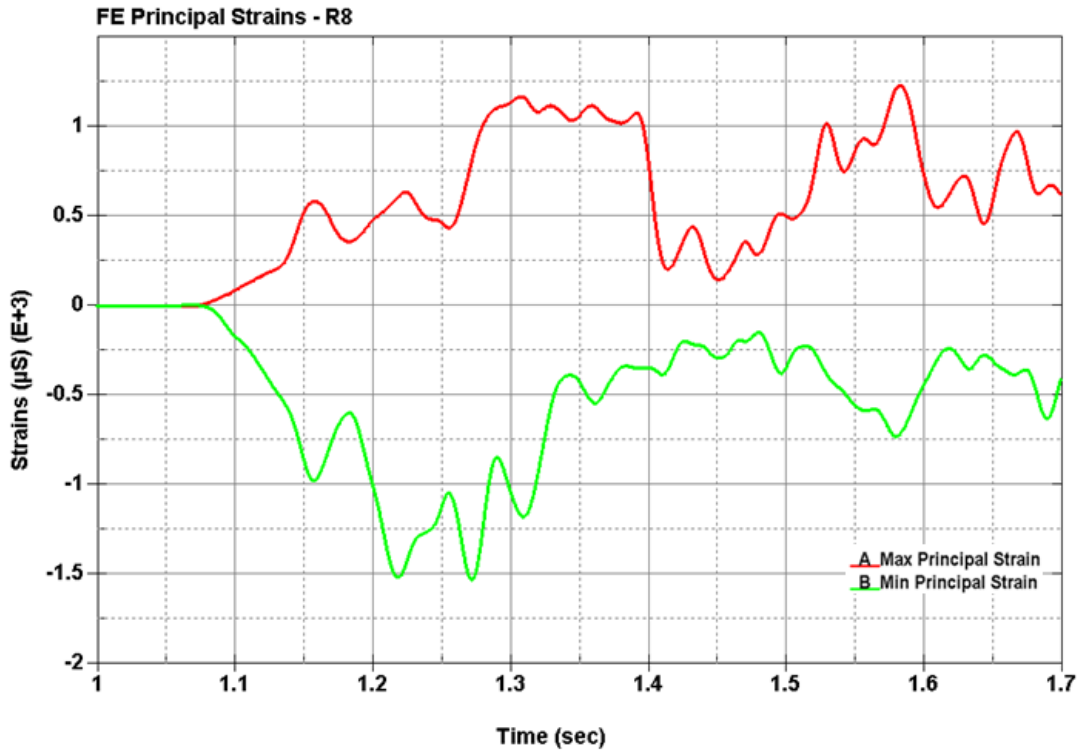

Principle Strains from LS-DYNA Simulation Location R8

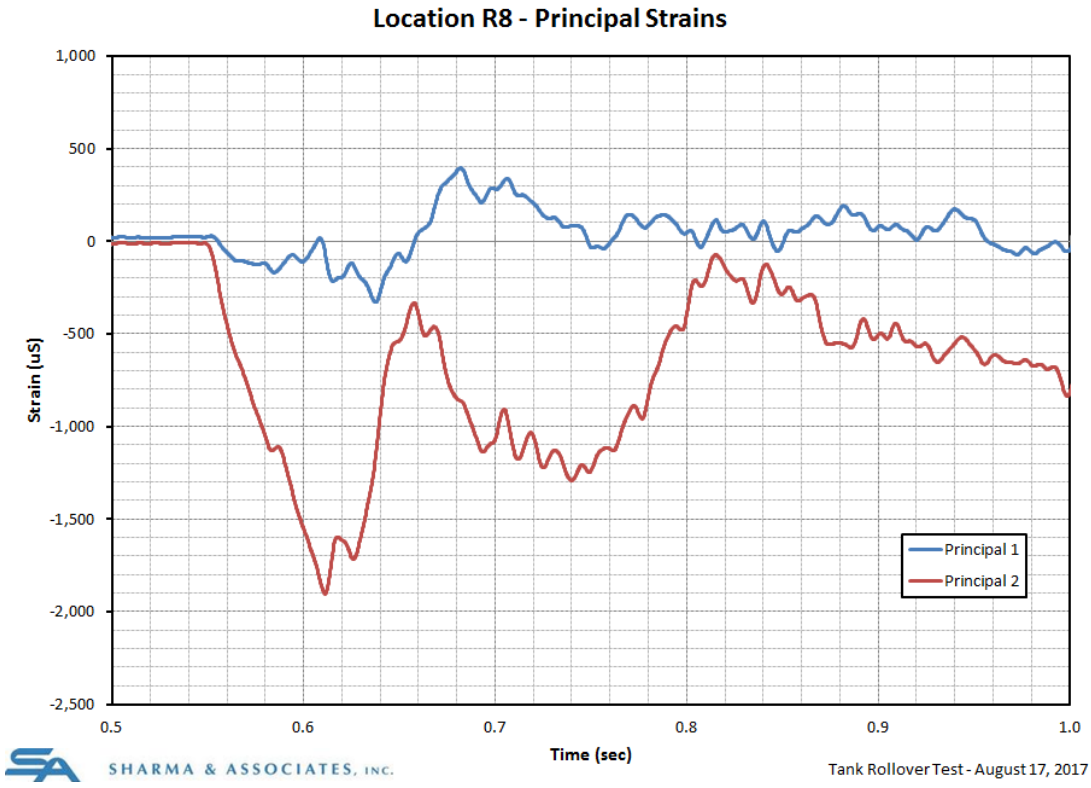

Principle Strains from Actual Test Location R8

Figure A6

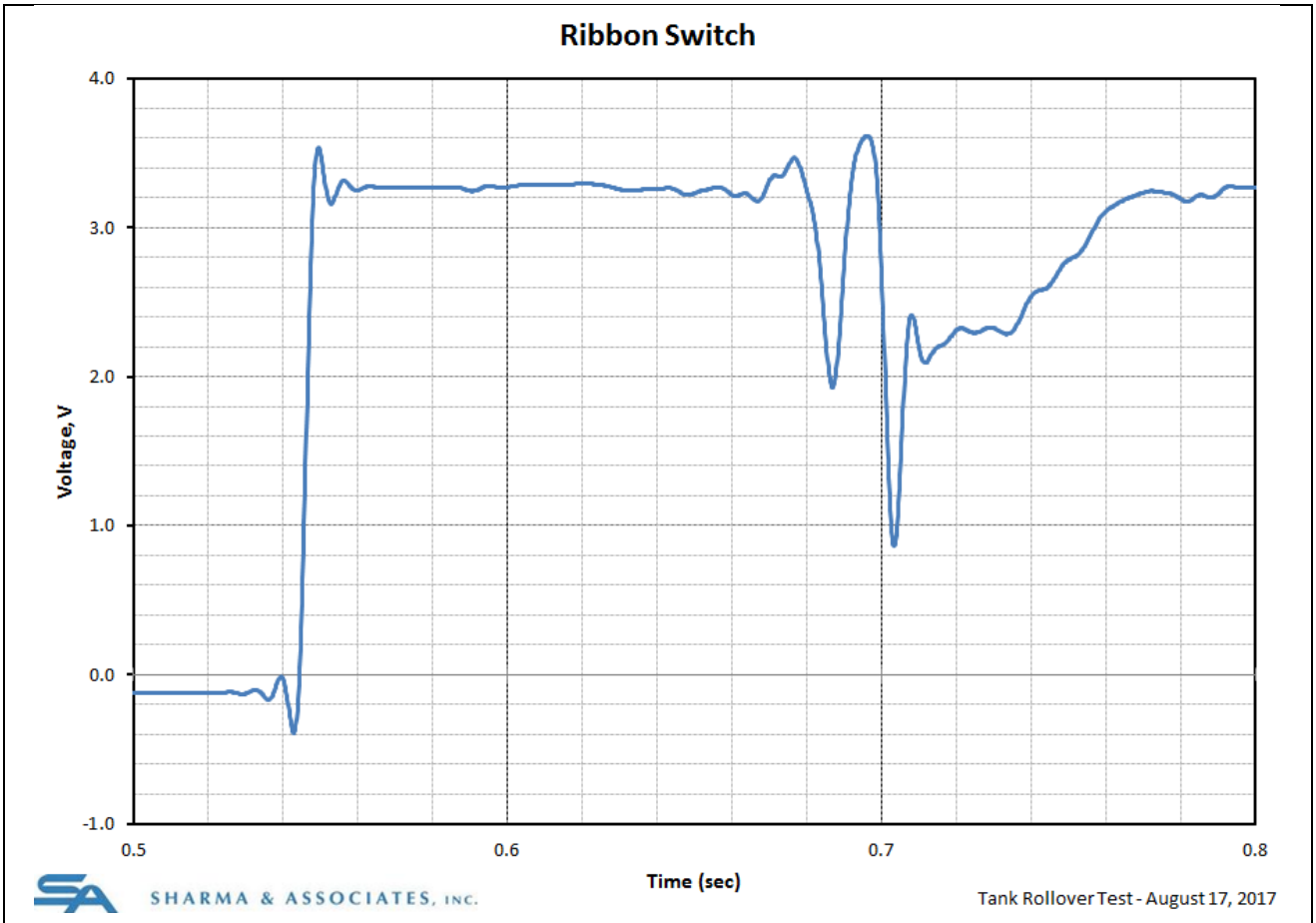

Time at Impact Shown by Ribbon Switch Output

Figure A7

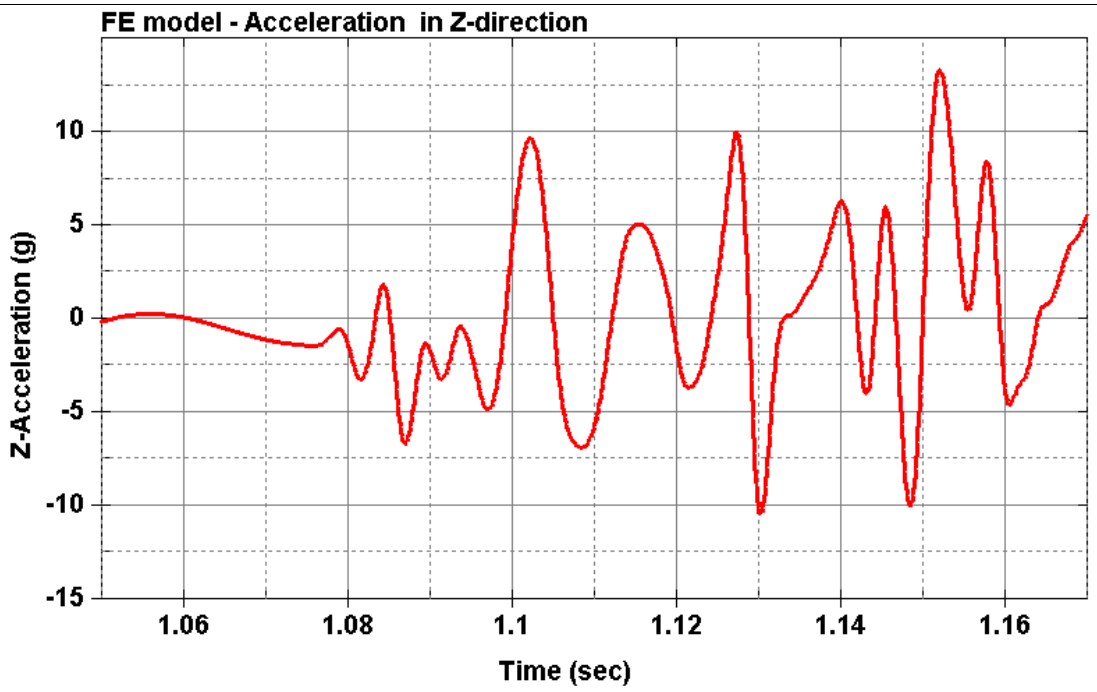

Z-direction Acceleration – LS DYNA Simulation

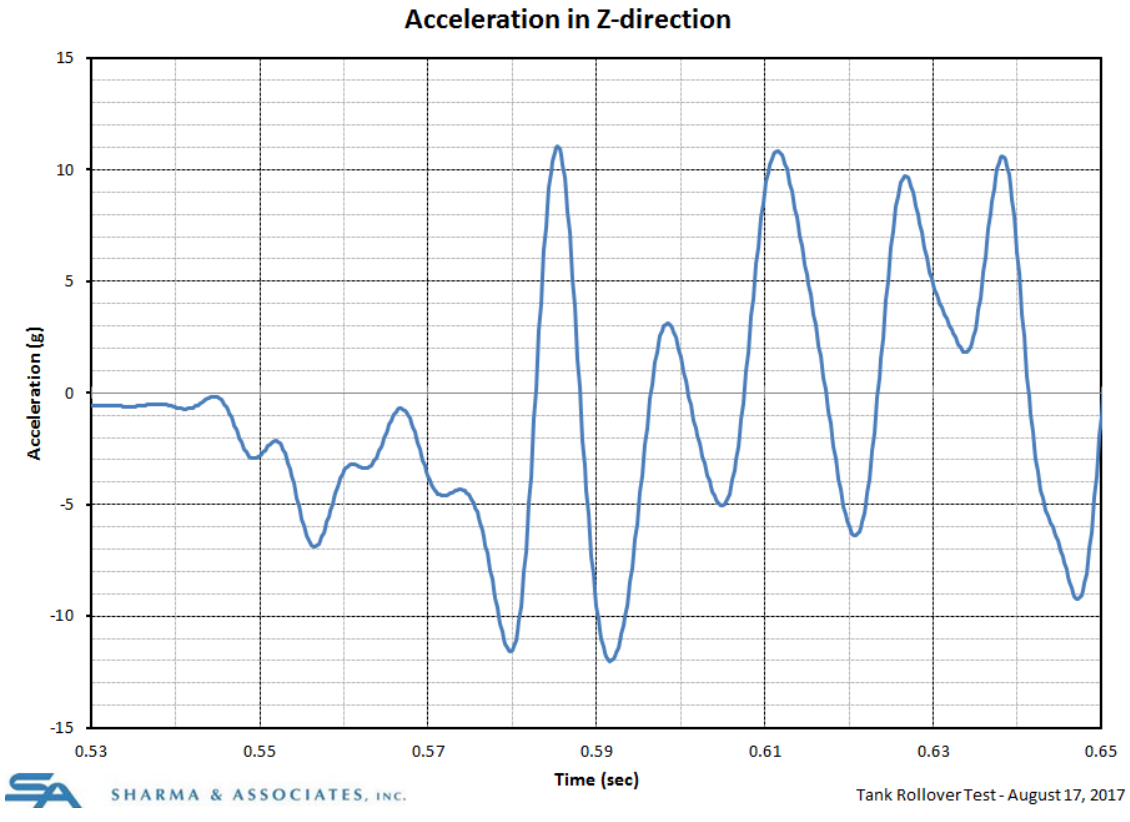

Z-direction Acceleration – Actual Test

Figure A8

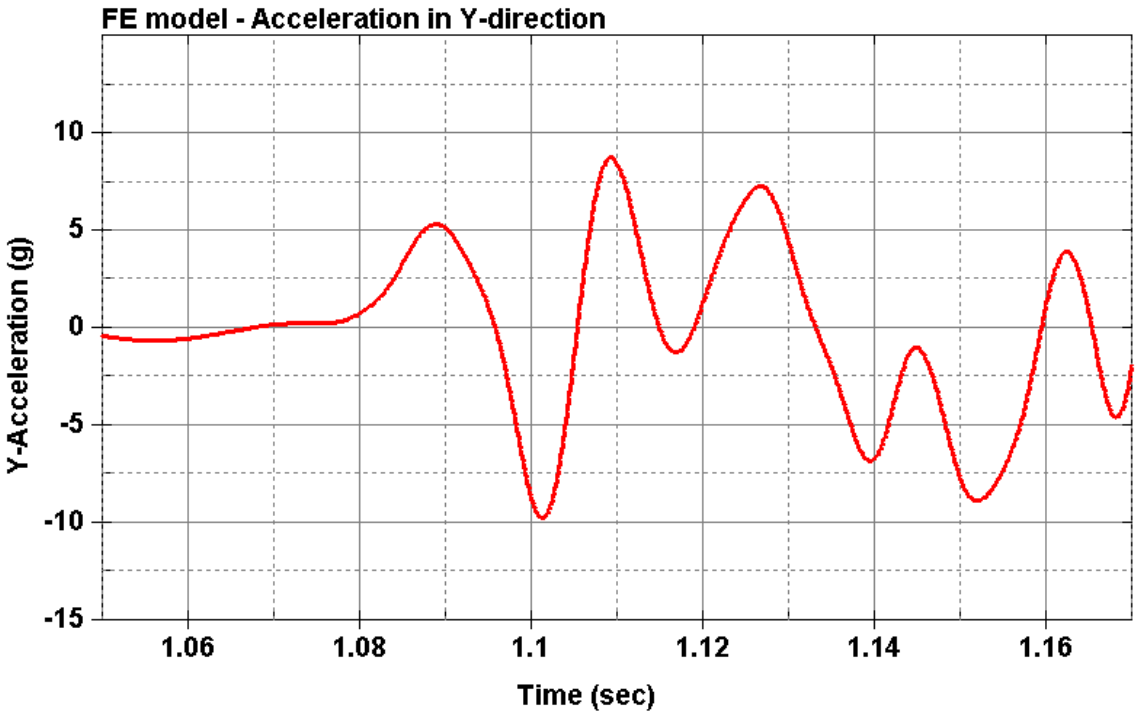

Y-direction Acceleration – LS DYNA Simulation

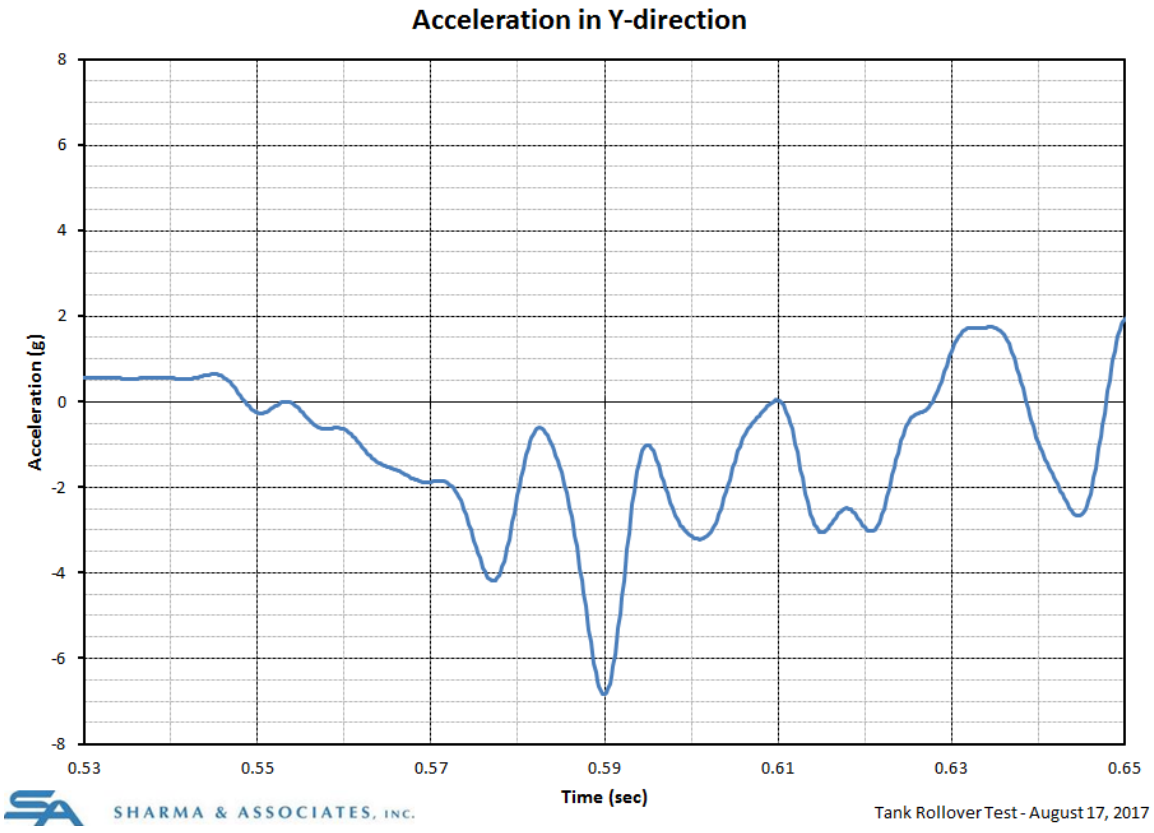

Y-direction Acceleration – Actual Test

Figure A9